Functional Specificity and Sex Differences in the Neural Circuits Supporting the Inhibition of Automatic Imitation

Darda, Kohinoor Monish; Butler, Emily; Ramsey, Richard

Journal of Cognitive Neuroscience

DOI:
10.1162/jocn_a_01261

Published: 01/06/2018

Peer reviewed version

Journal: JoCN

Title: **Functional Specificity and Sex Differences in the Neural Circuits Supporting the Inhibition of Automatic Imitation**

Running title: **Functional specificity and automatic imitation**

Kohinoor M. Darda*, Emily E. Butler* and Richard Ramsey

Wales Institute for Cognitive Neuroscience, School of Psychology, Bangor University, Bangor, Gwynedd, Wales, LL57 2AS, United Kingdom

Corresponding author: r.ramsey@bangor.ac.uk

* = Joint first authors

Key words: fMRI; domain specificity; imitation-inhibition.

Abstract

Although humans show an involuntary tendency to copy other people's actions, which builds rapport between individuals, we do not copy actions indiscriminately. Instead, copying behaviours are guided by a selection mechanism, which inhibits some actions and prioritises others. To date, the neural underpinnings of the inhibition of automatic imitation and differences between the sexes in imitation control are not well understood. Previous studies involved small sample sizes and low statistical power, which produced mixed findings regarding the involvement of domain-general and domain-specific neural architectures. Here, we used data from Experiment 1 (N=28) to perform a power analysis to determine the sample size required for Experiment 2 (N=50; 80% power). Using independent functional localisers and an analysis pipeline that bolsters sensitivity, during imitation control we show clear engagement of the multiple-demand network (domain-general), but no sensitivity in the theory-of-mind network (domain-specific). Weaker effects were observed with regard to sex differences, suggesting that there are more similarities than differences between the sexes in terms of the neural systems engaged during imitation control. In sum, neurocognitive models of imitation require revision to reflect that the inhibition of imitation relies to a greater extent on a domain-general selection system rather than a domain-specific system supporting social cognition.

Introduction

Human social interactions are guided by non-verbal cues, such as copying behaviours. In the last two decades, much research has investigated the involuntary tendency to copy other's actions - a phenomenon known as automatic imitation (Heyes 2011). Automatic imitation is thought to be beneficial in social situations because it develops affiliative attitudes, better co-operation, and feelings of closeness between interacting partners (Chartrand and Lakin, 2013). Prior neuroscience research has shown that imitation is supported by the mirror neuron system (MNS), a neural network engaged in perceiving and performing actions (Iacoboni et al. 1999; Iacoboni 2009; Rizzolati and Craighero 2004). Imitation, however, is unlikely to rely on a single cognitive or brain system (Southgate and Hamilton 2008). For example, in many circumstances, imitation is maladaptive, and requires inhibition (Newman-Norlund et al. 2007; van Schie et al. 2008; Cross et al., 2013; Cross & Iacoboni, 2014). In such situations, a selection mechanism is required to suppress the tendency to imitate and prioritise alternative actions (Brass et al. 2009). To date, studies investigating the neural mechanisms of imitation control have been limited by small sample sizes and low statistical power, which has produced mixed findings (Table 1). Further, no neuroscience research has investigated how individual differences such as sex modulate imitation control, even though behavioural research has shown that imitative tendencies vary as a function of sex (Butler, Ward, and Ramsey 2015; Dimberg 1990; Sonnby-Borgström et al. 2008). Across two functional magnetic resonance imaging (fMRI) experiments, which had higher statistical power and functional sensitivity than prior studies, we investigated the extent to which imitation inhibition relies on a domain-specific or domain-general neural network, which varies its response as a function of sex.

Much like cognitive science in general (Hirschfeld and Gelman 1994; Kanwisher 2010), inhibitory control research has focused on a neat division between domain-general and domain-specific mental operations. Domain-general inhibitory systems, which operate across multiple tasks, have been identified in dorsal frontoparietal cortices (Aron et al. 2014; Bunge et al. 2002; Hazeltine et al. 2007; Nee et al. 2007; Wager et al. 2005). This brain circuit has been labelled the multiple demand network (MD) network, due to its engagement in a diversity of mental operations (Duncan, 2010). By contrast, evidence from fMRI, neurostimulation and neuropsychological patient studies has suggested that a domain-specific circuit in an anterior portion of medial prefrontal cortex (mPFC) and right temporoparietal junction (rTPJ) operates during the inhibition of imitation (Brass et al., 2001; 2003; Klapper et al., 2014; Spengler et al., 2009; 2010; Santiesteban et al., 2012; Wang et al., 2011; Hogeveen et al., 2014; Santiesteban et al., 2015; Sowden & Catmur, 2015; Bardi et al., 2017). Beyond the control of imitation, mPFC and rTPJ have been consistently implicated in a variety of social cognition functions, which require distinguishing between self and other, as well as reasoning about other people's mental states (Theory of Mind, ToM; Amodio & Frith, 2006; Frith & Frith, 1999; van Overwalle, 2009; Saxe & Kanwisher, 2003). These results led to theorising that a key neural circuit for social cognition also regulates imitative tendencies (Brass et al., 2009).

Although theories of imitation control have developed that are based on functioning of the theory of mind network, evidence from fMRI studies that used a reaction time measure of imitation inhibition have not provided consistent support for the involvement of a domain-specific neural network (Table 1). The reaction time measure of imitation involves making finger movements while simultaneously watching compatible or

incompatible finger movements (Brass et al., 2000). The difference between reaction times in these two conditions (i.e. the general compatibility effect) has been argued to index imitative control as greater cognitive resources are required to inhibit movements that are incompatible to one's own responses (Brass & Heyes, 2005; Heyes, 2011). Approximately half of the fMRI studies using this paradigm failed to find engagement of rTPJ and anterior mPFC. In addition, a number of studies showed engagement of regions associated with the MD network including dorsal frontoparietal cortex, supplementary motor area (SMA) and anterior insula (Bien, Roebroeck, Goebel, & Sack, 2009; Crescentini, Mengotti, Grecucci, & Rumiati, 2011; Cross & Iacoboni, 2013; Marsh, Bird, & Catmur, 2016; Mengotti et al., 2012). Moreover, the most common measure of imitation interference is confounded by spatial compatibility or the tendency to respond faster to a stimulus when it is on the same side of space as the response (e.g. Simon 1969). In order to measure imitation interference independent of spatial compatibility effects, spatial and imitative processes need to be dissociated (Berthental et al. 2006; Boyer et al. 2012; Catmur and Heyes 2011; Cooper et al. 2012; Gowen et al. 2016; Wiggett et al. 2011; Marsh et al. 2016). Therefore, the extent to which imitation inhibition relies on domain-specific and domain-general architectures remains unclear. Indeed, no research to date has dissociated spatial from imitative processes and used a functional region of interest approach (fROI; Kanwisher 2010 Fedorenko et al. 2013). Using a fROI approach enables investigation of how functionally-defined brain circuits, such as the MD and ToM networks, operate during the control of imitation.

A further area of imitation research that has received little attention is the extent to which imitative control varies across individuals, especially between the sexes. It has been

argued that imitation is modulated by stable individual differences such as empathy (Chartrand and Lakin 2013) and sex (Butler et al. 2015; Sonnby-Borgström et al. 2008). Although it has been suggested that women excel across a range of social processes compared to men (Baron-Cohen 2002), only a limited number of studies have investigated sex differences in social cognition and the results are often mixed, do not replicate, or are specific to very select contexts or samples (Hyde 2014; Miller and Halpern 2014). Further, studies of sex differences in social cognition have mainly focused on emotional expression perception and mental state reasoning with little emphasis placed on imitation (Campbell et al., 2002; Thayer & Johnsen, 2000; Rahman et al., 2004; Krach et al., 2009; Russell et al., 2007).

A recent study that used a reaction time measure of imitation inhibition (Brass et al, 2000), showed that females showed a greater level of interference than males (Butler, Ward, & Ramsey, 2015). It is possible that this sex difference in imitation control may be mediated by empathy - females have been shown to be more empathetic compared to males (Baron-Cohen & Wheelwright, 2004; Christov-Moore et al., 2014). However, even though empathy has been associated with different types of imitation paradigms (Chartrand & Bargh, 1999; Müller et al., 2013; Sonnby- Borgström, Jönsson, & Svensson, 2003; Soonby-Borgström, 2002), the evidence to date suggests that there is no link between imitation, as measured by reaction times, and empathy (Butler et al., 2015; Genschow et al., 2017). In addition, in the study by Butler and colleagues (2015), it is unclear whether sex modulates the tendency to automatically imitate or the tendency to automatically respond in the same spatial location to the observed action. The former indicates a sex difference that is specifically tied to imitation control, while the latter might indicate a sex difference in

processes associated with resolving spatial conflict. More recent work also showed a greater interference effect for females compared to males (Genschow et al., 2017), as well as greater error rates for predominantly female samples than males (Cracco et al., in press). The imitation task used by Genschow and colleagues (2017) was controlled for left-right spatial compatibility, by presenting the stimulus hand orthogonal to the response. Even though this shows that the sex difference remains when spatial compatibility is reduced, it does not rule out the possibility of orthogonal spatial compatibility (Weeks & Proctor, 1990). More generally, sex differences have been found on a wide range of inhibitory control tasks including Flanker, Gaze-Cueing, Arrow-Cueing, Oddball, and Simon tasks, wherein females have been shown to require more cognitive resources than males to inhibit automatic response tendencies (Figure 1; Bayliss et al., 2005; Clayson et al., 2011; Rubia et al., 2010; Stoet, 2010; 2017). It is possible, therefore, that a domain-general system may underpin the sex differences observed across these tasks, including during imitation control, but no research to date has directly investigated this proposal.

Across two fMRI experiments, the current study investigated functional specificity and sex differences in imitation control. Several aspects of the experimental design provide grounds to extend current understanding in meaningful and concrete ways. First, this is the first study to use independent functional localisers to identify MD and ToM networks in single subjects and directly test the involvement of these networks in imitation control. By doing so, we can directly test hypotheses regarding the role of functionally-defined neural circuits (i.e., MD and ToM networks) and therefore minimise the reliance on reverse-inference to infer cognitive function based on anatomical localisation (Poldrack, 2006). Second, we used data from Experiment 1 to perform a power analysis to determine the

sample size required to achieve a desired level of power in Experiment 2. Given the inconsistent findings in prior studies, which had relatively small sample sizes, this multi-experiment approach made sure that our key experiment had over 80% power to detect expected effect sizes. Third, to avoid spatial compatibility confounds, in Experiment 2, we used a modified version of the imitation inhibition paradigm that allowed for an independent measure of spatial and imitative compatibility (Catmur & Heyes, 2011). If the inhibition of automatic imitation relies on a domain-specific neural architecture that is associated with social cognition, as proposed by Brass and colleagues (Brass et al., 2009), mPFC and rTPJ would be engaged in imitative control. In contrast, engagement of the MD network would suggest that domain general processes subserve imitation control. Further, the sex difference found previously (Butler et al. 2015) may be supported by differences in ToM or MD networks.

Materials and Methods

Overview of the experimental approach

Experiment 1 used a group-level whole-brain analysis, which provided the basis for power analyses that set up Experiment 2 as the critical experiment with high statistical power (80%). In Experiment 2, in order to increase sensitivity and functional resolution, we used independent localisers to identify key functional circuits (i.e. MD and ToM networks) and analyses were performed in single subjects to precisely quantify the consistency of network engagement across individuals (Kanwisher, 2010; Nieto-Castanon & Fedorenko, 2012). Group-level analyses require responses across individuals to overlap in individual voxels. In contrast, the fROI approach allows identification of corresponding functional

regions without the requirement of exact voxel overlap across individuals. Therefore, the exact same voxels need not be active across individuals, as long as voxels within a functionally-defined ROI are consistently active across individuals. Consequently, group level analyses may underestimate functional specificity, whereas fROI analyses can show increased sensitivity (Nieto-Castanon & Fedorenko, 2012). In addition, due to a constrained search volume, fROI analyses typically have higher statistical power than whole-brain analyses (Fedorenko et al., 2010; Saxe et al., 2006).

Experiment 1

Participants

28 participants (M_{age} = 23.96, SD_{age} =5.52; 14 females) participated for monetary compensation of £15. Participants gave informed consent in line with the guidelines set by the Research Ethics and Governance Committee of the School of Psychology at Bangor University, were right-handed, had normal or corrected-to-normal vision, and reported no history of neurological damage.

Design and procedure

All participants performed the imitation task inside the scanner. The participants also did four additional tasks in the same scanning session as part of another experiment. The scanning session started with the imitation task, followed by a run of a face perception task, a flanker task (Erikson & Erikson, 1974), another run of the face perception task, a dynamic face localiser (Pitcher et al., 2011), and a theory of mind localiser (Dodell-Feder et al., 2011). The order of the tasks was counterbalanced across participants such that out of

the 28 participants, 14 participants did the imitation task first, and 14 participants did the flanker task first, with the order of the other tasks remaining the same.

The Imitation Inhibition Task

The imitation task was based on a stimulus-response compatibility paradigm developed by Brass et al. (2000) consisting of observation and execution of finger lifting movements during fMRI scanning. Before the task, participants were instructed to hold down the 'blue' and 'yellow' buttons on the response box with their index and middle fingers respectively of the right hand. A number cue (either '1' or '2') was presented to participants, and they were asked to lift their index finger on presentation of the number '1' and the middle finger for the number '2.' Simultaneously, they also viewed an image of an index or middle finger lift of a left hand viewed from the third person perspective such that the fingers extended towards the participants. Thus, there were four trial types in an event-related design that led to two conditions – participants performing the same (congruent) or different (incongruent) finger movement to the observed hand image.

Each trial started with a fixation cross (500 ms) followed by a neutral hand (for a random inter-stimulus interval of 500, 700, or 1000 ms), and a hand image with an index/ middle finger lift, which stayed onscreen for 2000 ms irrespective of when the participant made the response. After 2000 ms, the next trial started immediately with a fixation cross (500 ms). In order to separately model the influence of individual events set closer together in time separately in an event-related design, the four trial types were pseudorandomized such that each trial type was preceded by each other trial type and by itself an equal number of times (Josephs & Henson, 1999; Wager & Nichols, 2003). There were 17 trials in each block. The first trial was used to set up the randomization sequence but excluded from

the analysis as it was not preceded by any other trial. The remaining 16 trials within a block were analysed and consisted of 8 trials per condition. Each run consisted of 5 blocks separated by a 3, 4, or 5 second fixation cross. All participants completed one run of the imitation task. Thus, there were 80 trials of interest (40 congruent and 40 incongruent).

Behavioural Data Analysis

Reaction time on the imitation inhibition task was measured as the time from number cue onset to when participants made a response. To ensure participants were engaging correctly with the task, participants who had less than 80% accuracy were removed. In addition, RTs more than 3SD away from the mean were excluded from the analyses. Further, trials on which participants made an 'error' were excluded from the analyses. Errors included an incorrect response, no response, a response after 2000 ms and pressing an invalid key. The general compatibility effect was calculated as the RT difference between incompatible and compatible trials. A one-sample t-test was performed to verify the presence of a general compatibility effect. A one-tailed independent sample t-tests was performed to determine if the compatibility effect was greater for females than males. Mean differences, 95% confidence intervals (CI), and Cohen's d (Cohen, 1992) are reported for all effects of interest. For the one sample t-test, Cohen's d_z was calculated as mean difference divided by the standard deviation of the sample (Lakens, 2013). For the independent samples t-test, Cohen's d was calculated as mean difference between the two groups divided by the pooled standard deviation (Cohen, 1992).

fMRI Data Analysis

Data acquisition

Participants were placed supine in a 3-Tesla Philips MRI scanner using a SENSE 32 channel phased array coil. They were requested to avoid head motion during the scanning session and were presented stimuli on a computer screen placed behind the scanner made visible by a mirror attached to the head coil. Responses on the task were recorded with the help of a button box that recorded reaction times. 35 axial slices were acquired in an ascending order using a T2*-weighted EPI sequence. The reference slice for slice time correction was the slice acquired in the middle of the sequence (slice 17). Parameters are as follows: voxel size = 3 x 3 x 4 mm; repetition time (TR) = 2000ms; echo time (TE) = 30ms; flip angle = 90 degrees; slice thickness = 4mm; slice gap = 0.8mm; FOV: 230 x 230 x 167 mm^3. 174 volumes were collected for the imitation task.

Four dummy scans collected at the beginning of each run of the task were not included in any analyses. A high-resolution T1-weighted anatomical image was also collected with the following parameters: TR = 12ms; TE = 3.5ms, flip angle = 8 degrees; number of axial slices = 170; voxel size = $1mm^3$; FOV: 250 x 250 x $170mm^3$.

Data Preprocessing and General Linear Model

Functional images were preprocessed in SPM-8. Data were realigned, unwarped, and corrected for slice timing. Data were normalised to the MNI template with a resolution of $3mm^3$ and images were spatially smoothed (8mm).

For the imitation task, a design matrix was fit for each participant with three regressors: one each for the coorect trials of the two conditions, and one for the 'new' trials (i.e. the first trial of each block). The new trials were not used in any further analyses. Stimulus onsets were time-locked to the presentation of the number cue with a duration of zero seconds and convolved with the standard haemodynamic response function.

Whole-brain analyses

Contrast images (incompatible > compatible) were calculated at the single subject level for the imitation inhibition task in order to identify regions of the brain showing a compatibility effect. Group level contrast images were created from these single-subject contrast images in order to identify regions that were consistently engaged for the compatibility effect across the sample using one-sample t-tests. In order to identify a neural signature of the sex difference in imitation inhibition, a sex*compatibility ANOVA was computed [Female (incompatible > compatible) > Male (incompatible > compatible)] as females have been shown to have a higher compatibility effect than males in the imitation task (Butler et al., 2015). For all analyses, contrast images were taken to the group level and thresholded using a voxel-level threshold of $p < .001$ and a voxel-extent of 10 voxels. Correction for multiple comparisons was performed at the cluster level (Friston et al., 1994) with clusters that survive correction for multiple corrections using a family-wise error (FWE) correction ($p < .05$) (shown in bold font in Table 2(A) and (B); see Results). Clusters of activity were identified with the SPM Anatomy toolbox (Eickhoff et al., 2005).

Experiment 2

Participants

55 participants (M_{age} = 22.04, SD_{age} = 3.70; 27 females) were recruited from the Bangor community and were either reimbursed with £15 or 3 course credits for their participation. Informed consent was obtained in line the guidelines set by the Research Ethics and Governance Committee of the School of Psychology at Bangor University. All participants were right-handed, did not have dyslexia or dyspraxia, were not on any medication, did not report neurological damage, and had normal or corrected-to-normal

vision. The sample size was determined by a power analysis based on Experiment 1 data (see Results).

Design and procedure

Each participant performed three tasks inside the scanner – the Automatic Imitation task, a Theory of Mind (ToM) network localiser task, and a Multiple Demand (MD) network localiser task. The order of the tasks was as follows: two runs of the MD network localiser task were interspersed between three runs of the imitation task in order to offset boredom, followed by two runs of the ToM task. The ToM task was always presented at the end to reduce the likelihood that belief reasoning during the ToM task would influence performance in the imitation task. The order was the same for all participants. Participants also completed a 50 item International Personality Item Pool (IPIP) questionnaire (Donnellan et al., 2006; Goldberg, 1992) (unrelated to the current study), and a stimulus rating form where they were asked to rate the hand stimulus from the imitation task as either male, female, or neutral. The entire session lasted approximately 1.5 hours, with 60 minutes inside the scanner. All stimulus presentation was coded in Matlab 2015b, and presented with PsychToolBox 3.0.6.

The Imitation Inhibition Task

The automatic imitation task was similar to the one used in Experiment 1 but with two changes. First, we used a different hand stimulus, which was rated as sex-neutral by observers. The sex of the hand was an important consideration in order to minimise the possibility of an own-sex bias while exploring sex differences in imitation inhibition. As such, we conducted pilot work that asked observers to evaluate a range of hand stimuli in terms of masculinity and femininity and we selected the most sex-neutral stimulus (see

Supplementary Information, Development of Stimuli). We only used one hand stimulus in order to simplify the design space. Although using one sex-neutral hand stimulus provided greater experimental control, it may have harmed our ability to study or elicit sex differences. Future work could probe this further by varying the sex of the stimulus and/or by using more sex-typical stimuli.

The second change that we made was to calculate an imitative compatibility effect independent of spatial compatibility (Catmur & Heyes, 2011). To do so, participants viewed an image of an index or middle finger lift of either a right or left hand, but always responded with their right hand. Using right and left-hand images produced eight trial types and four main conditions of interest (see Figure 2 (A)). For example, when cued to lift their index finger while observing a left-hand index finger lift, the observed movement is both imitatively compatible (same finger), as well as spatially compatible (same side of space to the executed movement). In contrast, when observing a right-hand index finger lift, the participant's response is imitatively compatible (same finger) but it is not on the same side of space (they are spatially incompatible). Thus, participants performed the same (imitatively compatible) or different (imitative incompatible) finger movement on the same (spatially compatible) or different (spatially incompatible) side of space to the observed finger movement, giving rise to the following four conditions:

1. Imitatively and spatially compatible
2. Imitatively and spatially incompatible
3. Imitatively compatible and spatially incompatible
4. Imitatively incompatible and spatially compatible

Sequencing information and pseudo-randomisation was the same as Experiment 1. There were 65 trials in each block. The first trial was used to set up the randomization sequence but excluded from the analysis as it was not preceded by any other trial. The remaining 64 trials were analysed, consisting of 16 trials per condition. Each run consisted of 2 blocks separated by a 3 second fixation cross. All participants completed three runs of the imitation task. In total, there were 384 trials of interest, 96 per condition. Experiment 2, therefore, had more than twice the number of trials per condition than Experiment 1.

Localiser tasks

The Multiple Demand Network Localiser

In order to identify regions of the MD network, a verbal Working Memory (WM) task was used (Fedorenko, et al., 2011). Participants were asked to remember the sequence in which either four (easy condition) or eight (hard condition) digit sequences were presented on screen (see Figure 2 (B)). After each trial, participants had to choose between two digit sequences presented numerically, one of which matched the sequence in which the digits were presented as words. Feedback was provided as to whether they answered correctly or incorrectly. The *hard>easy* contrast has been found to robustly activate regions of the MD network (Fedorenko et al., 2011; 2013). Each run consisted of 10 experimental blocks (each 34 seconds long) and 6 fixation blocks (each 16 seconds long). The total experiment lasted for 436 seconds. Each participant completed two runs of the WM task.

The Theory of Mind Localiser

In order to localise brain regions involved in mental state reasoning, we used a paradigm developed by Doddell-Feder and colleagues (2011; http://saxelab.mit.edu/superloc.php). This localiser task (see Figure 2 (C)) includes 20

stories, each describing a false representation. 10 stories included out-of-date beliefs (the false belief condition) and the other 10 included out-of-date physical representations (photographs/maps; the false photograph condition). The *False Belief>False Photograph* contrast has been shown in prior work to robustly activate regions involved in mentalising (Dufour et al., 2013). All trials consisted of a story (10 s), followed by a true or false question (4 s). Each story was separated by a 12-s rest period. The order of the stories and conditions was the same for all participants. Each participant completed two runs of this task: 5 trials of each condition were presented in each run.

Behavioural Data Analysis

RT and accuracy were recorded in the same way as Experiment 1. Compatibility effects were calculated as follows: spatial compatibility = spatially incongruent trials – spatially congruent trials; imitative compatibility = imitatively incongruent trials – imitatively congruent trials. Behavioural data were analysed in the same fashion as Experiment 1 only separately for imitative and spatial compatibility effects. The main aim of the experiment was to test for the presence of imitative and spatial compatibility effects, as well as for differences between the sexes (females > males). Hence, we used a one-sample t-test in order to verify the presence of spatial and imitative compatibility effects, and a one-tailed independent samples t-test in order to test whether females showed a higher spatial/imitative compatibility effect than males.

fMRI Data Analysis

Data Acquisition

Data acquisition procedures were the same as Experiment 1. There were 249 volumes collected for the imitation task, 219 for the MD network localiser, and 136 for the ToM localiser for each run.

Data Preprocessing and General Linear Model

All MRI data were preprocessed in SPM-8. Data were realigned, unwarped, and corrected for slice timing. Data were normalised to the MNI template with a resolution of $3mm^3$. Normalising to a common space instead of the individual's native anatomical space, allows for comparisons with previous studies (relying on the common space) and is preferred when definition of fROIs is based on group-constrained functional data (Nieto-Castanon & Fedorenko, 2012). Images were spatially smoothed (8mm).

For the imitation task, a design matrix was fit for each participant with five regressors: one each for the correct trials of the four conditions, and one for 'new' trials (i.e. the first trial of each block). Stimulus onsets were time-locked to the presentation of the number cue with a duration of zero seconds and convolved with the standard haemodynamic response function. Contrast images were calculated for each individual subject in order to identify regions of the brain showing a spatial (spatially incompatible > spatially compatible) or imitative (imitatively incompatible > imitatively compatible) compatibility effect.

For the localiser tasks, the design matrix consisted of regressors for each experimental condition ('Belief' and 'Photo' for the ToM localiser, and 'Hard' and 'Easy' for the MD localiser). The onset and duration of each condition was specified and convolved with the standard haemodynamic response function. Contrast images were then calculated

for each individual subject in order to identify regions that responded to cognitive demand (Hard > Easy) and mentalising (Belief > Photo).

Definition of group-constrained subject-specific (GSS) analyses

For the GSS analyses, the spm_ss toolbox was used, which runs in SPM using Matlab (http://web.mit.edu/evelina9/www/funcloc.html). The Group-constrained Subject-Specific (GSS) approach developed by Fedorenko et al. (2010) and Julian et al. (2012) was used to define functional regions of interest for each participant. These fROIs were defined using 1) each individual's activation map for the localiser tasks, and 2) group-constraints or masks. These masks refer to a set of "parcels", which demarcate areas in the brain where prior work has been shown to exhibit activity for the localiser contrasts.

Two sets of fROIs were defined (Figure 3): MD network fROIs that have been known to exhibit activity for a variety of cognitive control tasks (Duncan et al., 2010; Fedorenko et al., 2013) and ToM network fROIs that support mentalising and have been specifically implicated for imitation inhibition (Saxe & Kanwisher, 2003; Brass et al., 2009). For the ToM network, four parcels were derived from a group-level map from 462 participants for the False Belief > False Photograph contrast (Dufour et al., 2013). These regions included the dorsal, medial, and ventral prefrontal cortex (DMPFC, MMPFC, VMPFC), and the right temporo-parietal junction (rTPJ). For the MD network, we used 16 parcels derived from a set of functional parcels created by Idan Blank based on a probabilistic overlap map from 197 participants (available at: https://evlab.mit.edu/funcloc/download-parcels). These included areas in bilateral superior and inferior parietal lobules (SPL, IPL), inferior parietal sulcus (IPS), inferior and middle frontal gyrus (IFG, MFG), precentral gyrus (PrecG), insula (Ins), and the supplementary motor area (SMA). These areas were chosen for two reasons:

1) they were part of the MD network (Fedorenko et al., 2013) and 2) they have been shown to respond in prior work to the specific type of interference control of relevance to the current study (Marsh et al., 2016; also see Experiment 1).

For each individual, these masks were used to constrain the selection of subject-specific fROIs. For each individual, for the ToM network mask, the Belief>Photo contrast was used and the top 10% of voxels (based on t-values) within each parcel were defined as that individual's fROI. Similarly, for the MD network mask, each individual's top 10% of voxels (based on t-values) in the Hard>Easy contrast were defined as that individual's fROI. Using the top 10% of voxels, rather than a fixed threshold (e.g., all voxels with $p < 0.001$), ensures a constant size of each fROI across individuals (Blank, Kanwisher, & Fedorenko, 2014). We also ran the analyses using a fixed threshold ($p<0.001$, uncorrected) and found the same pattern of results (see Supplementary Tables S1.1 and S1.2). All analyses reported below are based on the top 10% of voxels based on the localiser data. Percent signal change (PSC) values were extracted from all fROIs. For the main analysis, all runs of the localiser tasks were used to define fROIs in each individual. Responses in these fROIs were estimated for spatial and imitative compatibility effects.

In a supplementary analysis, responses to the localiser contrasts were also estimated in order to ensure that all the fROIs showed the expected response with respect to the localiser contrasts i.e. the ToM network showed a robust Belief>Photo and the MD network showed a robust Hard>Easy effect. For these localiser analyses, an across-runs cross validation approach was used (Nieto-Castanon & Fedorenko, 2012) to ensure that data used for defining fROIs was independent of data used for estimating response (Kriegeskorte et al., 2009).

As implemented in GSS, statistical tests were performed on the PSC values using standard Student's t-tests. One-sample t-tests were performed to investigate the response of the MD and ToM network fROIs to spatial and imitative compatibility effects. Based on prior behavioural findings, which showed greater RT interference for females than males during imitation inhibition (Butler et al., 2015), we expected to observe sex differences in those regions that also show simple compatibility effects. That is, we expected brain regions that were generally involved in spatial and/or imitative control to show sex differences. As such, we only investigated sex difference in those fROIs that showed spatial or imitative compatibility effects. To do so, one-tailed independent samples t-tests were performed that tested for greater engagement for females than males. False Discovery Rate (FDR) multiple comparison correction ($p<.05$) was used to correct for the number of fROIs in each functional network.

Results

Experiment 1

Behavioural results

A one-sample t-test confirmed a general compatibility effect (Mean = 80.02, SE = 8.19), t (27) = 9.77, p = <.001, 95% CI (63.22, 96.82), Cohen's d_z = 1.85. A one-tailed independent samples t-test showed no differences between males (Mean = 70.94, SE = 13.30) and females (Mean = 89.10, SE = 9.43), t (26) = 1.114, p = .138, 95% CI (-45.96), Cohen's d = 0.42. All participants had >80% accuracy and hence all were included in the analysis. Trials on which participants made an incorrect response (0.95%), did not make a

response or responded after 2000 ms (0.52%) or pressed an invalid key or responded too fast (0.09%) were excluded from the analyses.

fMRI results

In a whole-brain analysis, compatibility effects (general incompatible > general compatible) were observed in dorsomedial frontal cortex and bilaterally in dorsolateral frontal and parietal cortices (Figure 4 (A); Table 3(A)). A small volume correction (SVC) using MD and ToM network parcels was performed in order to restrict the search area to ToM and MD networks. Using the MD network SVC, results showed widespread activation of frontal and parietal regions, which survived correction for multiple comparisons (Figure (4A, Ci)). In contrast, using the ToM network SVC, no clusters survived correction for multiple comparison and only rTPJ showed a compatibility effect at more lenient threshold ($p<.001$, uncorrected) (see Supplementary Tables S2.1 and S2.2). Anterior mPFC did not show the general compatibility effect even at this more lenient threshold.

The sex*compatibility interaction revealed clusters in left superior parietal lobule extending into postcentral gyrus and a further cluster in the cerebellum (Figure 4 (B); Table 3(B)). No clusters emerged following a SVC analysis using the MD and ToM network masks, which demonstrates that the clusters emerging from the sex*compatibility interaction do not overlap with the MD or ToM networks (see Supplementary Tables S2.1 and S2.2; Figure 4 (Cii) and (Dii)).

Power Analysis

We set up Experiment 1 as a pilot in order to estimate the appropriate sample size for our critical experiment (Experiment 2). To this end, a power analysis was performed using the fMRIpower software package (fMRIpower.org; Mumford & Nichols, 2008). We

performed the power analysis as follows: first, a whole brain map of the imitation task general compatibility effect (Incompatible>Compatible) from Experiment 1 was entered into fMRIpower. Next, two ROIs were identified: the MD network (Duncan, 2010) and the ToM network (Saxe & Kanwisher, 2003). The MD and ToM network masks used were the same as in Experiment 2 (see Materials and Methods). As recommended, we corrected the alpha value by the number of ROIs (0.05/2 = 0.025) before performing power analyses (Mumford, 2012).

Results from these power analyses showed that testing 50 participants in Experiment 2 would provide 80% power to detect effects as large as (or larger than) the average effect size that was observed across all nodes in the MD network in Experiment 1 (Cohen's d = 0.4, Mean Signal Change = 0.23, SD = 0.58). We did not have the same level of power to detect smaller effects than these, such as those observed in the ToM network in Experiment 1. Indeed, the effects in the ToM network in Experiment 1 were so small that we would have needed an impractically large sample size to achieve 80% power. As such, in Experiment 2 we decided to test participants until we had 50 usable datasets.

Design differences between Experiments 1 and 2 are worth considering when interpreting these power calculations because we may be underestimating the power of our design in Experiment 2. The toolbox used to run power calculations (fmripower.org) can only estimate power for a future experiment with the same design as the current dataset (Mumford & Nichols, 2008). However, the designs of Experiment 1 and 2 differed in two ways. First, Experiment 1 measured a general compatibility effect, whereas in Experiment 2, we broke this effect down into spatial and imitative compatibility effects. Second, Experiment 2 had more than double the amount of trials per condition as Experiment 1.

Therefore, the primary contrast used to determine power was not identical to the contrast used in Experiment 2, but due to a greater number of trials per condition to estimate the effects of interest, we may underestimate power in Experiment 2. Given the lack of sex differences in Experiment 1 in our regions of interest, we did not have sufficient power to convincingly investigate neural differences between males and females in Experiment 2. However, given our *a priori* predictions regarding sex, we continue to report sex difference analyses throughout the paper.

Experiment 2

Behavioural Results

The hand stimulus used in Experiment 2 for the imitation inhibition task was perceived as 'neutral' by most participants ($Mean_{rating}$ = 5.20, SD_{rating} = 2.04; rated on a scale of 1 to 9, where 1 = most masculine, 5 = neutral, and 9 = most feminine). To ensure participants were engaging correctly with the task, runs on which participants had less than 80% accuracy (2 runs of one participant) were removed. In addition, RTs more than 3SD away from the mean (2 runs of one participant and one run of another participant) were excluded from the analyses. Further, trials on which participants made an incorrect response (1.52%), did not make a response or responded after 2000 ms (0.61%) or pressed an invalid key (0.22%) were also excluded from the analyses. Figure 5 shows the imitative and spatial compatibility effects for both the sexes. For RT data see Supplementary Table S3.

Spatial compatibility. A one-sample t-test confirmed a spatial compatibility effect (Mean = 41.94, SE = 2.87), t (54) = 14.618, p = <.001, 95% CI (36.19, 47.69), Cohen's d_z = 1.97. A one-tailed independent samples t-test evidenced a greater spatial interference effect

for females (Mean = 50.98, SE = 3.67) as compared to males (Mean = 33.20, SE = 3.75), t (53) = -3.38, p = <.001, 95% CI (24.01), Cohen's d = 0.91.

Imitative compatibility. A one-sample t-test showed a significant imitative compatibility effect (Mean = 15.37, SE = 2.86), t (54) = 5.37, p < .001, 95% CI (9.63, 21.11) Cohen's d_z = 0.72. There was no significant difference between males (Mean = 15.62, SE = 4.39) and females (Mean = 15.11, SE = 3.73), t (53) = 0.09, p = .930, 95% CI (-15.78), Cohen's d = 0.02.

fMRI Results

Five participants were excluded from the fMRI analyses because of less than 80% accuracy in two runs of the imitation task and the MD network localiser task (N=1), and excessive head motion (N=4; displacement > 4mm) in all runs of the imitation task and/or all runs of either of the localiser tasks. Thus, the final sample consisted of 50 participants (M_{age} = 22.26; SD_{age} = 3.71; 24 females). From these 50 participants, two sessions of the imitation task were also excluded for one participant due to excessive head motion and one participant's data for one session of the imitation task could not be used because the data file was corrupted.

Localiser tasks

All fROIs showed the predicted responses to the localiser contrasts (as estimated using data not used for defining ROIs; see Methods). All the MD Network fROIs showed a robust Hard>Easy effect (ts > 9.13, ps < .0001) and ToM Network fROIs showed a robust Belief>Photo effect (ts > 5.70, ps < .0001). For responses for each individual fROI separately, see Supplementary Tables S4.1 (MD) and S4.2 (ToM).

The Automatic Imitation Task

GSS Analyses

Figure 6 shows the mean percent signal change for each fROI over baseline in the MD and ToM networks for spatial and imitative compatibility.

Multiple Demand Network fROIs

Spatial Compatibility. All 16 fROIs of the MD Network showed a spatial compatibility effect (ts>1.8, ps < .04; Figure 6 (A), Table 3), which survived correction for multiple comparisons (p<.05, FDR corrected). The mean percent signal change across the MD network for spatial compatibility was 0.70, SD = 1.66, Cohen's d = 0.42. No significant differences were found between males and females in percent signal change values in any of the fROIs (ts < 1.6, ps > .1), except right SPL which approached significance (p = .062) (Figure 7 (A)).

Imitative Compatibility. None of the 16 MD Network fROIs showed an imitative compatibility effect, which survived correction for multiple comparisons (all ps>.05, FDR-corrected). 5 MD network fROIS showed an imitative compatibility effect at an uncorrected threshold (ts > 1.95, ps < .05). These fROIS include bilateral IPL, bilateral IPS, and the right IFG (Figure 6 (A), Table 3). Four further fROIS showed an imitative compatibility effect that approached significance, which included left IFG (p=.07), right SPL, right MFG and right PrecG (p=.06). The mean percent signal change across the MD network for imitative compatibility was 0.54, SD = 2.06, Cohen's d = 0.26. There was no significant difference between males and females in any of these fROIs (ts < 1.5, ps > .08) (see Figure 7(B)).

Theory of Mind Network fROIs

None of the ToM network fROIs showed imitative (ts < 1.3, ps > .50) or spatial (ts < 1.6, ps > .06) compatibility effects, even at an uncorrected significance threshold (Figure 6

(B), Table 4). rTPJ showed a spatial compatibility effect that approached significance (p=0.065). The mean percent signal change across the ToM network for spatial compatibility was -0.16, SD = 1.88, Cohen's d = -0.08, and for imitative compatibility was -0.32, SD = 2.02, Cohen's d = -0.16.

Whole-brain analyses

For completeness, and for use in future meta-analyses, we also computed group-level whole-brain analyses separately for general, spatial, and imitative compatibility effects, as well as for sex*compatibility interactions (see Supplementary Table S4).

Open science

Data for Experiments 1 and 2 are freely available online including behavioural and fROI data (osf.io/45x6z), as well as whole-brain t-maps (https://neurovault.org/collections/EPSIHNQQ/).

Discussion

The current study provides the most robust neuroimaging evidence to date for a lack of functional specificity in the neural circuits supporting the inhibition of automatic imitation. With higher statistical power and functional sensitivity than prior studies, across two experiments the results demonstrate that imitation inhibition engages a domain-general neural network as opposed to a brain network that supports social cognition. As such, models of imitation control need updating to include an increased role for domain-general processes and a reduced or altered role for domain-specific processes. Further, in terms of behaviour, females showed a higher spatial but not imitative compatibility effect than males. However, there was no sex difference in the neural mechanisms underlying spatial

or imitation control, which suggests that further exploration of sex differences in inhibitory control is required.

Functional specificity in imitation inhibition

Our findings show that brain regions that are engaged in a verbal working memory task, which are associated with the operation of the MD network (Duncan, 2010; Fedorenko et al., 2013), are also engaged during spatial and imitative conflict resolution. These results support the involvement of a domain-general cognitive and neural system during the control of imitation. By contrast, brain regions that are engaged in a belief reasoning task, which are associated with the operation of the theory of mind network (Frith & Frith, 1999; Saxe & Kanwisher, 2003; van Overwalle, 2009), show no engagement during the inhibition of imitation. As such, we provide no evidence for domain-specificity in cognitive and neural systems that control imitation.

Brass and colleagues (2009) proposed that in the context of imitation control, rTPJ is involved in self/other distinction and mPFC enforces the self-generated action over the observed action. Our findings are inconsistent with the hypothesis that a specific neural system related to social cognition is engaged in the inhibition of automatic imitative tendencies. mPFC and rTPJ have both been implicated in imitation inhibition by some studies (Brass et al., 2005; 2009; Spengler et al., 2009; Wang et al., 2011). In contrast, other studies found engagement of mPFC only (Brass et al., 2001; Cross et al., 2013) or of domain general regions rather than mPFC and rTPJ (Bien, Roebroeck, Goebel, & Sack, 2009; Crescentini, Mengotti, Grecucci, & Rumiati, 2011; Cross & Iacoboni, 2013; Marsh, Bird, & Catmur, 2016). In both experiments in the current study, we had larger sample sizes than prior experiments and, in Experiment 2, we had sufficient statistical power to be confident

in detecting effects as large as previously observed in mPFC and rTPJ, should they exist. Taken together with prior findings (Table 1), we suggest that during the inhibition of imitation, the consistency of mPFC and rTPJ engagement across individuals is low, whereas the consistency of MD network engagement across individuals is relatively high.

These results have potential implications for self-other control theories of social cognition more generally. Mostly based on imitation research, which previously suggested that mPFC and rTPJ are engaged in imitation inhibition, self-other control is thought to be a candidate mechanism for a diverse set of social functions (Brass et al., 2009; de Guzman et al., 2016; Sowden & Shah, 2014). For example, self-other control processes have been linked to autism, empathy, and theory-of-mind (Spengler et al., 2009; de Guzman et al., 2016; Sowden & Shah, 2014). However, recent behavioural findings, which used larger sample sizes than prior work and meta-analytical approaches, do not support the view that the control of imitation varies as a function of social disposition as indexed by autistic-like traits and empathy (Butler et al., 2015; Cracco et al., in press; Genschow et al., 2017). In light of these recent behavioural results, the lack of engagement of mPFC and rTPJ in the current study raises an important question about the reliance of imitation inhibition on a self-other distinction. One possibility is that instead of a distinctly social mechanism (Boyer et al., 2012; Bertenthal & Scheutz, 2013), inhibiting imitative tendencies may involve the same cognitive processes that are used when inhibiting other non-social external influences (Heyes, 2011; Cooper et al., 2013).

Alternatively, the engagement of mPFC and rTPJ during self-other control processes may be more complicated than what current models of social cognition suggest. Indeed, a small number of neurostimulation studies have shown that modulation to rTPJ can

influence performance on RT measures of imitation (Hogeveen et al., 2014; Sowden & Catmur, 2015). In addition, mPFC and rTPJ have been found to be involved in the modulation of automatic imitation. For example, Klapper et al. (2014) found a higher response in rTPJ when an interaction partner looked human and was believed to be human compared to when neither of these animacy cues were present. Wang and colleagues (2011) demonstrated that mPFC had a top-down influence on other brain circuits during social modulation of imitation via direct gaze. These studies suggest that mPFC and/or rTPJ may have a regulatory role, be sensitive to social context, and be functionally connected to other regions during the inhibition of automatic imitation. Indeed, regions that do not show direct engagement in a cognitive process of interest have been known to have a regulatory influence on other regions that are directly engaged (Burnett & Blakemore, 2009). In line with this proposal, Cross and colleagues (2013) suggested that imitation control involves top-down regulation between a domain-general cognitive control network, and a domain-specific network relevant for imitation. More generally, research from other domains of social cognition shows growing evidence for higher complexity and functional interplay within and between so-called domain-specific and domain-general networks (Baetens et al., 2014; Spunt & Adolphs, 2015; Quadflieg et al., 2011; Zaki et al., 2010). These studies suggest that models including neat divisions between these networks may be an overly simplistic characterisation of mental function (Barrett, 2012; Michael & D'Ausilio, 2014). Much like social cognition in general, therefore, imitation control may be best explained by interactions between component functional circuits, which themselves need not be domain-specific (Spunt & Adolphs, 2017). A crucial direction for future research is testing for more

complex models of imitation, which may involve connectivity in and between regions of the MD and ToM networks.

An important point to note, however, is that any conclusions made regarding possible domain-specificity of mPFC and rTPJ are based on the assumption that mPFC and rTPJ are at least partly specialised for social cognition (Brass et al., 2009). Recent evidence suggests that mPFC and rTPJ may be functionally versatile in the sense that they show general cognitive properties, which may not be specific to social cognition (Alexander & Brown, 2011; Carter & Huettel, 2013; de la Vega et al., 2016; Dugue et al., 2017; Schurz et al., 2017; Schuwerk et al., 2017; Yarkoni et al., 2011). Thus, the argument that the engagement of mPFC and rTPJ in imitation-inhibition may be specific to social cognition might need further validation. Additionally, social cognition itself has been broken down in 'bottom-up' and 'top-down' domains (Zaki & Oschner, 2012). The bottom-up domain refers to pre-reflective processes that are fast and stimulus driven whereas the top-down domain maps on reflective, cognitively laborious and flexible processes (Bohl & van der Boss, 2012). When extended to imitation control, prior research has consistently implicated regions involved in top-down control for automatic imitation (Brass et al., 2009). However, recent studies suggest that that imitation control (and social cognition more broadly) relies on interactions between bottom-up and top-down processes (Cross & Iacoboni, 2014; Christov-Moore, Conway, & Iacoboni, 2017; Bohl & van der Boss, 2012). Thus, another important avenue for future research would be to investigate imitation control based on bottom-up and top-down processes and their interactions, rather than considering these processes as mutually exclusive.

Nonetheless, results from the current study remain clear: the basic imitation inhibition mechanism engages the multiple demand network, which has been consistently associated with domain-general processes (Duncan, 2010). Given the mixed findings in prior imitation studies (Table 1), as well as psychology and neuroscience more generally (Open Science Framework, 2015; Button et al., 2013), future fMRI research may also consider reliability and reproducibility as key concerns in imitation research and consider the possible use of fROI as a means to quantify consistency across individuals.

Sex differences in imitation inhibition

This study is the first to investigate sex differences in the neural mechanisms that inhibit imitation. The behavioural data demonstrated that females show a greater spatial but not imitative compatibility effect than males. This result extends prior behavioural research on sex differences, which did not separate spatial (or orthogonal spatial) from imitative responses in imitation control (Butler et al., 2015; Genschow et al.,2017). The result is also consistent with reports in a wide range of non-social inhibitory control tasks, which show similar sex differences (Figure 2; Bayliss et al., 2005; Clayson et al., 2011; Rubia et al., 2010; Stoet, 2010; 2017). All these tasks share a common feature – they require the inhibition of a response to a task-irrelevant spatial feature in order to enforce a task-relevant response. Taken together, this pattern of results suggests that response inhibition relating to spatial conflict differs between the sexes, rather than a process that is tied to the control of imitation. An alternative possibility is that the difference between the sexes for spatial compatibility is larger than for imitative compatibility, and we were unable to detect the imitative effect behaviourally. Future research will have to probe these possibilities further.

Given the proposed role of MD and ToM networks in imitation control, we anticipated sex differences in one or both of these networks. The neuroimaging data, however, demonstrated no sex differences in the ToM or MD networks in either experiment. Further, even though regions outside of our regions of interest mediated the sex difference in Experiment 1, these regions were not consistently engaged differently for males and females in Experiment 2. Thus, based on data across both experiments, our best estimate is that univariate analyses, which assess the magnitude of BOLD response, do not show large effects of sex in MD or ToM neural networks. This being said, there does seem to be a trend for greater engagement in the MD network for females compared to males for both spatial and imitative effects, but this does not survive our statistical thresholding (Figure 7). As a consequence, we are cautious to interpret this null result as we did not have the same level of statistical power to detect sex differences as we did to detect simple compatibility effects. Indeed, it remains a possibility that small univariate effects exist or that the sex difference is underpinned by more complex neural organisation. Future studies that use connectivity measures (Sporns, 2005) or multi voxel pattern analysis (Normal et al., 2006; Kriegeskorte, 2008) may show increased sensitivity and be better able to capture the complexity of neural organization that we are aiming to measure.

Limitations

The primary limitation of the current work is that we studied a relatively simple model of brain organisation based on univariate measures. Given the mixed evidence from prior studies regarding imitation control (Table 1), we felt it was an important step to first establish the extent to which general and specific systems were engaged in a univariate

manner. By doing so, we aimed to build an appropriate foundation for future work to build upon. Moreover, as we only identified the MD and ToM networks, it is possible that neural regions outside our key networks may play a role in imitation inhibition or mediate the sex difference in spatial response inhibition or imitation control. Even though our whole-brain analyses showed no consistent effects outside of our fROIs, this only shows that there was no univariate engagement of extended brain regions. We thus acknowledge that we have tested a relatively simple model of brain organisation that is likely to underestimate the complexity of neural processes associated with social and cognitive mechanisms such as imitation control. Future work may consider interactions between general and specific systems and more complex, multivariate measures of brain organisation such as MVPA.

A second limitation regards the functional localisation approach used to identify the ToM and MD networks in Experiment 2. The validity of the fROI approach is based on assumptions about the functional processes that are engaged by the localisers used to identify fROIs. For example, different ToM localisers may engage partly non-overlapping aspects of the ToM network (Spunt & Adolphs, 2014; Schaafsma, Pfaff, Spunt, & Adolphs, 2015). Therefore, our conclusions about the role of ToM and MD networks are limited to the type of localiser paradigms that we used in the current study. Future research that uses different functional partitions of these networks would be instructive.

A final potential limitation is that the order of tasks in Experiment 2 could have influenced our results. We ordered the tasks such that ToM localiser was always performed at the end, but MD task was interspersed between imitations runs to offset boredom. We arranged blocks in this manner because we were primarily concerned that asking people to perform a belief reasoning task would introduce a social bias to treat the person (hand

image) in an artificially more social/belief reasoning manner during the imitation-inhibition task. We did not share the same level of concern that performing a memory task, which we used to localise the domain—general system, would introduce a memory or "cognitive control" bias to the imitation-inhibition task. However, we cannot rule out the possibility in the current experiment that the MD task influenced the way the imitation task was performed. This being said, we did get the same results in Experiment 1, when the MD task was not performed before the imitation task. As such, although possible, we find it unlikely that task order had a meaningful impact on our results in Experiment 2.

Funding

This work was funded by a grant from the Economic and Social Research Council (grant number: ES/K001884/1 to R.R.). We thank Ruud Hortensius for comments on a previous version of the manuscript.

References

Alexander, WH, & Brown, JW. 2011. Medial prefrontal cortex as an action-outcome predictor. Nature Neuroscience, 14(10), 1338–1344.

Amodio DM, Frith CD. 2006. Meeting of minds: the medial frontal cortex and social cognition. Nat Rev Neurosci. 7:268-277.

Aron AR, Robbins TW, Poldrack RA. 2014. Inhibition and the right inferior frontal cortex: one decade on. Trends Cogn Sci. 18:177-185.

Bardi, L., Gheza, D., & Brass, M. 2017. TPJ-M1 interaction in the control of shared representations: new insights from tDCS and TMS combined. NeuroImage, 146:734-740.

Baron-Cohen S. 2002. The extreme male brain theory of autism. Trends Cogn Sci. 6:248-254.

Baron-Cohen, S., & Wheelwright, S. (2004). The empathy quotient: an investigation of adults with Asperger syndrome or high functioning autism, and normal sex differences. Journal of autism and developmental disorders, 34(2), 163-175.

Barrett HC. 2012 A hierarchical model of the evolution of human brain specializations. Proc Natl Acad Sci. 109:10733-10740.

Bayliss AP, di Pellegrino G, Tipper SP. 2005. Sex differences in eye gaze and symbolic cueing of attention. The Quarterly Journal of Experimental Psychology. 58A:631-650.

Bertenthal BI, Longo MR, Kosobud A. 2006. Imitative response tendencies following observation of intransitive actions. Journal of Experimental Psychology: Human Perception and Performance. 32:210.

Bertenthal, B. I., & Scheutz, M. (2013). In praise of a model but not its conclusions: Commentary on Cooper, Catmur, and Heyes (2012). Cognitive science, 37(4), 631-641.

Bien N, Roebroeck A, Goebel R, Sack AT. 2009. The brain's intention to imitate: the neurobiology of intentional versus automatic imitation. Cereb Cortex. 19:2338-51.

Blank I, Kanwisher N, Fedorenko E. 2014. A functional dissociation between language and multiple-demand systems revealed in patterns of BOLD signal fluctuations. J Neurophysiol. 112:1105-18.

Bohl, V., & van den Bos, W. 2012. Toward an integrative account of social cognition: marrying theory of mind and interactionism to study the interplay of Type 1 and Type 2 processes. Frontiers in Human Neuroscience, 6:274.

Boyer TW, Longo MR, Bertenthal BI. 2012. Is automatic imitation a specialized form of stimulus–response compatibility? Dissociating imitative and spatial compatibilities. Acta Psychologica. 139:440-8.

Brass M, Bekkering H, Wohlschlager A, Prinz W. 2000. Compatibility between observed and executed finger movements: comparing symbolic, spatial, and imitative cues. Brain and Cognition, 44: 124-143.

Brass M, Zysset S, von Cramon DY. 2001. The inhibition of imitative response tendencies. NeuroImage, 14:1416-1423.

Brass M, Derrfuss J, Matthes-von Cramon G, von Cramon DY. 2003. Imitative response tendencies in patients with frontal brain lesions. Neuropsychology, 17:265-271.

Brass M, Derrfuss J, von Cramon DY. 2005. The inhibition of imitative and overlearned responses: a functional double dissociation. Neuropsychologia, 43:89-98.

Brass, M., & Heyes, C. 2005. Imitation: is cognitive neuroscience solving the correspondence problem? Trends Cogn Sci, 9:489-495.

Brass M, Ruby P, Spengler S. 2009. Inhibition of imitative behaviour and social cognition. Philos Trans R Soc Lond B Biol Sci. 364:2359-67.

Bunge SA, Hazeltine E. Scanlon MD, Rosen AC, Gabrieli JDE. 2002. Dissociable contributions of prefrontal and parietal cortices to response selection. NeuroImage. 17:1562-1571.

Butler EE, Ward R, Ramsey R. Investigating the relationship between stable personality characteristics and automatic imitation. PloS one. 10:e0129651.

Burnett S, & Blakemore SJ. 2009. Functional connectivity during a social emotion task in adolescents and in adults. European Journal of Neuroscience. 29:1294–301.

Button KS, Ioannidis JP, Mokrysz C, Nosek BA, Flint J, Robinson ES, Munafò MR. 2013. Power failure: why small sample size undermines the reliability of neuroscience. Nat Rev Neurosci. 14:365-376.

Campbell R, Elgar K, Kuntsi J, Akers R, Terstegge J, Coleman M, Skuse D. 2002. The classification of ‘‘fear’’ from faces is associated with face recognition skill in females. Neuropsychologia, 40: 575–584.

Carter R.M. & S.A. Huettel. 2013. A nexus model of the temporal– parietal junction. Trends Cogn. Sci. (Regul. Ed.) 17:328–336.

Catmur C, Heyes C. 2011. Time course analyses confirm independence of imitative and spatial compatibility. Journal of experimental psychology. Human perception and performance. 37:409-21.

Chartrand TL, Lakin JL. 2013. The antecedents and consequences of human behavioural mimicry. Ann Rev Psych. 64:285-308.

Christov-Moore, L., Simpson, E. A., Coudé, G., Grigaityte, K., Iacoboni, M., & Ferrari, P. F. 2014. Empathy: Gender effects in brain and behavior. Neuroscience & Biobehavioral Reviews, 46:604-627.

Christov-Moore, L., Conway, P., & Iacoboni, M. 2017. Deontological Dilemma Response Tendencies and Sensorimotor Representations of Harm to Others. Frontiers in integrative neuroscience, 11:34.

Clayson PE, Clawson A, Larson MJ. 2011. Sex differences in electrophysiological indices of conflict monitoring. Biological Psychology. 87:282-289.

Cohen, J. 1992. A power primer. Quantitative Methods in Psychology. 112:155-159.

Cooper, R. P., Catmur, C., & Heyes, C. 2012. Are automatic imitation and spatial compatibility mediated by different processes? Cogn Sci. 37:605–30.

Cracco E, Bardi L, Desmet C, Rigoni D, Radkova I, Deschrijver E, Genschow O, De Coster L, Brass M. Automatic Imitation: A Meta-Analysis. In press. Psychological Bulletin.

Crescentini C, Mengotti P, Grecucci A, Rumiati RI. 2011. The effect of observed biological and non-biological movements on action imitation: an fMRI study. Brain research. 1420:80-92.

Cross KA, Iacoboni M. 2013. Optimised neural coding? Control mechanisms in large cortical networks implemented by connectivity changes. Human Brain Mapping. 34:213-25.

Cross, K. A., Torrisi, S., Losin, E. A. R., & Iacoboni, M. 2013. Controlling automatic imitative tendencies: interactions between mirror neuron and cognitive control systems. Neuroimage, 83:493-504.

Cross, K. A., & Iacoboni, M. 2014. To imitate or not: Avoiding imitation involves preparatory inhibition of motor resonance. Neuroimage, 91:228-236.

de Guzman M, Bird G, Banissy MJ, Catmur C. 2016. Self–other control processes in social cognition: from imitation to empathy. Phil. Trans. R. Soc. B. 371(1686):20150079.

de la Vega A, Chang LJ, Banich MT, Wager TD, Yarkoni T. 2016. Large-scale meta-analysis of human medial frontal cortex reveals tripartite functional organization. Journal of Neuroscience. 36(24):6553-62.

Dimberg U, Lundquist LO. 1990. Gender differences in facial reactions to facial expressions. Biol Psychol. 30:151-159.

Dodell-Feder D, Koster-Hale J, Bedny M, Saxe R. 2011. fMRI item analysis in a theory of mind task. Neuroimage. 55:705-712.

Donnellan MB, Oswald FL, Baird BM, Lucas RE. 2006. The mini-IPIP scales: tiny-yet-effective measures of the Big Five factors of personality. Psychological assessment. 18:192-203.

Downing PE, Jiang Y, Shuman M, Kanwisher N. 2001. A cortical area selective for visual processing of the human body. Science. 293:2470-3.

Dufour N, Redcay E, Young L, Mavros PL, Moran JM, Triantafyllou C, Gabrieli JD, Saxe R. 2013. Similar brain activation during false belief tasks in a large sample of adults with and without autism. PloS One. 8:e75468.

Dugué L, Merriam EP, Heeger DJ, Carrasco M. 2017. Specific Visual Subregions of TPJ Mediate Reorienting of Spatial Attention. Cerebral Cortex 1–16.

Duncan J. 2010. The multiple-demand (MD) system of the primate brain: mental programs for intelligent behaviour. Trends Cogn Sci. 14:172-9.

Eickhoff SB, Stephan KE, Mohlberg H, Grefkes C, Fink GR, Amunts K, Zilles K. 2005. A new SPM toolbox for combining probabilistic cytoarchitectonic maps and functional imaging data. Neuroimage. 25:1325–1335.

Eklund A, Nichols TE, Knutsson H. 2016. Cluster failure: Why fMRI inferences for spatial extent have inflated false-positive rates. Proceedings of the National Academy of Sciences of the United States of America 113:7900–7905.

Erikson BA, Erikson CW. 1974. Effects of noise letters upon the identification of a target letter in a nonsearch task. Perception and Psychophysics. 16:143-149.

Fedorenko E, Hsieh PJ, Nieto-Castañón A, Whitfield-Gabrieli S, Kanwisher N. 2010. New method for fMRI investigations of language: defining ROIs functionally in individual subjects. Journal of neurophysiology. 104:1177-94.

Fedorenko E, Duncan J, Kanwisher N. 2013. Broad domain generality in focal regions of frontal and parietal cortex. Proc Natl Acad Sci. 110:16616-21.

Friston KJ, Worsley KJ, Frackowiak RSJ, Mazziotta JC, Evans AC. 1994. Assessing the significance of focal activations using their spatial extent. Human Brain Mapping. 1:210-220.

Frith CD, Frith U. 1999. Interacting minds--a biological basis. Science. 286:1692-1695.

Genschow, O., van Den Bossche, S., Cracco, E., Bardi, L., Rigoni, D., & Brass, M. 2017. Mimicry and automatic imitation are not correlated. PloS one, 12(9), e0183784.

Goldberg, LR. 1992. The development of markers for the Big-Five factor structure. Psychological Assessment, 4, 26-42.

Gowen E, Bolton E, Poliakoff E. 2016. Believe it or not: Moving non-biological stimuli believed to have human origin can be represented as human movement. Cognition. 146:431-8.

Hazeltine E, Poldrack R, Gabrieli JDE. 2007. Neural activation during response competition. J Cogn Neurosci. 12:118-129.

Heyes C. 2011. Automatic imitation. Psychological bulletin. 137:463.

Hirschfeld LA, Gelman SA. 1994. Mapping the mind: Domain specificity in cognition and culture. Cambridge University Press.

Hogeveen J, Obhi SS, Banissy MJ, Santiesteban I, Press C, Catmur C, Bird G. 2014. Task-dependent and distinct roles of the temporoparietal junction and inferior frontal cortex in the control of imitation. Social Cognitive and Affective Neuroscience, 10:1003-1009.

Hyde JS. 2014. Gender similarities and differences. Annual review of psychology. 65:373-98.

Iacoboni M, Woods RP, Brass M, Bekkering H, Mazziotta JC, Rizzolatti G. 1999. Cortical mechanisms of human imitation. Science. 286:2526-2528.

Iacoboni M. 2009. Neurobiology of imitation. Curr Opin Neurobiol. 19:661-665.

Josephs O, Henson RN. 1999. Event-related functional magnetic resonance imaging: modelling, inference and optimization. Philosophical Transactions of the Royal Society of London B: Biological Sciences, 354:1215–1228.

Julian JB, Fedorenko E, Webster J, Kanwisher N. 2012. An algorithmic method for functionally defining regions of interest in the ventral visual pathway. Neuroimage. 60:2357-64.

Kanwisher N. 2010. Functional specificity in the human brain: a window into the functional architecture of the mind. Proc Natl Acad Sci. 107:11163-70.

Klapper A, Ramsey R, Wigboldus D, Cross ES. 2014. The Control of Automatic Imitation Based on Bottom-Up and Top-Down Cues to Animacy: Insights from Brain and Behavior. J Cogn Neurosci., 26: 2503-2513.

Krach S, Blumel I, Marjoram D, Lataster T, Krabbendam L, Weber J, van Os J, Kircher T. 2009. Are women better mindreaders? Sex differences in neural correlates of mentalizing detected with functional MRI. BMC Neuroscience. 10.

Kriegeskorte N, Simmons WK, Bellgowan PS, Baker CI, 2009. Circular analysis in systems neuroscience: the dangers of double dipping. Nat. Neurosci. 12:535–540.

Kriegeskorte N, Mur M, Bandettini P. 2008. Representational similarity analysis-connecting the branches of systems neuroscience. Frontiers in systems neuroscience. 2:4.

Lakens, D. (2013). Calculating and reporting effect sizes to facilitate cumulative science: a practical primer for t-tests and ANOVAs. *Frontiers in psychology*, *4*.

Marsh LE, Bird G, Catmur C. 2016. The imitation game: Effects of social cues on 'imitation' are domain-general in nature. NeuroImage. 139:368-75.

Michael J, D'Ausilio A. 2015. Domain-specific and domain-general processes in social perception–A complementary approach. Consciousness and cognition. 36:434-437.

Mengotti P, Corradi-Dell'Acqua C, Rumiati RI. 2012. Imitation components in the human brain: an fMRI study. Neuroimage. 59:1622-30.

Miller DI, Halpern DF. 2014. The new science of cognitive sex differences. Trends Cogn Sci. 18:37-45.

Müller, B. C., Leeuwen, M. L., Baaren, R. B., Bekkering, H., & Dijksterhuis, A. 2013. Empathy is a beautiful thing: Empathy predicts imitation only for attractive others. Scandinavian journal of psychology, 54(5), 401-406.

Mumford JA, Nichols TE. 2008. Power calculation for group fMRI studies accounting for arbitrary design and temporal autocorrelation. Neuroimage. 39:261-8.

Mumford JA. 2012. A power calculation guide for fMRI studies. Social cognitive and affective neuroscience. 7:738-42.

Nee DE, Wager TD, Jonides J. 2007. Interference resolution: Insights from a meta-analysis of neuroimaging tasks. Cogn Affect Behav Neurosci. 7:1-17.

Newman-Norlund RD, van Schie HT, van Zuijlen AM, Bekkering H. 2007. The mirror neuron system is more active during complementary compared with imitative action. Nat Neurosci. 10:817-819.

Nieto-Castañón A, Fedorenko E. 2012. Subject-specific functional localisers increase sensitivity and functional resolution of multi-subject analyses. Neuroimage. 63:1646-69.

Norman KA, Polyn SM, Detre GJ, Haxby JV. 2006. Beyond mind-reading: multi-voxel pattern analysis of fMRI data. Trends in cognitive sciences. 10:424-30.

Peelen MV, Downing PE. 2005. Selectivity for the human body in the fusiform gyrus. Journal of neurophysiology 93:603-608.

Pitcher D, Dilks DD, Saxe RR, Triantafyllou C, Kanwisher N. 2011. Differential selectivity for dynamic versus static information in face-selective cortical regions. Neuroimage, 56:2356-2363.

Poldrack RA. 2006. Can cognitive processes be inferred from neuroimaging data? Trends in cognitive sciences, 10(2):59-63.

Quadflieg S, Flannigan N, Waiter GD, Rossion B, Wig GS, Turk DJ, Macrae CN. 2011. Stereotype-based modulation of person perception. Neuroimage. 57:549–557.

Rizzolatti G, Craighero L. 2004. The mirror-neuron system. Annu Rev Neurosci. 27:169-192.

Rubia K, Hyde Z, Halari R, Giampietro V, Smith A. 2010. Effects of age and sex on developmental neural networks of visual-spatial attention allocation. NeuroImage. 51:817-827.

Russell TA, Tchanturia K, Rahman Q, Schmidt U. 2007. Sex differences in theory of mind: A male advantage on Happé's "cartoon" task. Cognition and Emotion. 21:1554–1564.

Santiesteban I, Banissy MJ, Catmur C, Bird G. 2012. Enhancing Social Ability by Stimulating Right Temporoparietal Junction. Curr Biol. 22: 2274-2277.

Santiesteban, I., Banissy, M. J., Catmur, C., & Bird, G. 2015. Functional lateralization of temporoparietal junction–imitation inhibition, visual perspective-taking and theory of mind. European Journal of Neuroscience, 42(8), 2527-2533.

Saxe R, Kanwisher N. 2003. People thinking about thinking people: the role of the temporo-parietal junction in "theory of mind". Neuroimage. 19:1835-42.

Saxe R, Brett M, Kanwisher N. 2006. Divide and conquer: a defense of functional localisers. Neuroimage. 30:1088-96.

Schurz M, Tholen MG, Perner J, Mars RB, Sallet J. 2017. Specifying the brain anatomy underlying temporo-parietal junction activations for theory of mind: A review using probabilistic atlases from different imaging modalities. Human brain mapping.

Schuwerk T, Schurz M, Müller F, Rupprecht R, Sommer M. 2017. The rTPJ's overarching cognitive function in networks for attention and theory of mind. Social cognitive and affective neuroscience. 12(1):157-168.

Simon JR. 1969. Reactions toward the source of stimulation. Journal of experimental psychology. 81:174.

Schaafsma SM, Pfaff DW, Spunt RP, Adolphs R. 2015. Deconstructing and reconstructing theory of mind. Trends in cognitive sciences, 19(2), 65-72.

Sonnby–Borgström, M. 2002. Automatic mimicry reactions as related to differences in emotional empathy. Scandinavian journal of psychology, 43(5), 433-443.

Sonnby-Borgström, M., Jönsson, P., & Svensson, O. (2003). Emotional empathy as related to mimicry reactions at different levels of information processing. Journal of Nonverbal behavior, 27(1), 3-23.

Sonnby-Borgström MA, Jönsson P, Svensson O. 2008. Gender differences in facial imitation and verbally reported emotional contagion from spontaneous to emotionally regulated processing levels. Scand J Psychol. 49:111-22.

Southgate V, Hamilton AF. 2008. Unbroken mirrors: Challenging a theory of autism. Trends Cogn Sci. 12:225-229.

Sowden S, & Shah P. 2014. Self-other control: a candidate mechanism for social cognitive function. Frontiers in human neuroscience. 8:789.

Sowden S, Catmur C. 2015. The role of the right temporoparietal junction in the control of imitation. Cerebral Cortex, 25:1107-1113.

Spengler S, von Cramon DY, Brass M. 2009. Control of shared representations relies on key processes in mental state reasoning. Human Brain Mapping. 30:3704-3718.

Spengler S, von Cramon DY, Brass M. 2010. Resisting motor mimicry: Control of imitation involves processes central to social cognition in patients with frontal and temporo-parietal lesions. Social Neuroscience, 5: 401-416.

Sporns O, Tononi G, Kötter R. 2005. The human connectome: a structural description of the human brain. PLoS Comp Biol. 1:e42.

Spunt, RP, Adolphs, R. 2014. Validating the why/how contrast for functional MRI studies of theory of mind. Neuroimage, 99:301-311.

Spunt RP, Adolphs R. 2015. Folk Explanations of Behavior: A Specialized Use of a Domain-General Mechanism. Psychological Science. 26: 724–736.

Spunt, RP, Adolphs R. 2017. A new look at domain specificity: insights from social neuroscience. Nature Reviews Neuroscience, 18(9):559.

Stoet G. 2010. Sex differences in the processing of flankers. The Quarterly Journal of Experimental Psychology. 63: 633-638

Stoet G. 2017. Sex differences in the Simon task help to interpret sex differences in selective attention. Psychological research.81:571-81.

Thayer JF, Johnsen BH. 2000. Sex differences in judgement of facial affect: a multivariate analysis of recognition errors. Scandinavian Journal of Psychology, 41:243–246.

van Schie HT, van Waterschoot BM, Bekkering H. 2008. Understanding action beyond imitation: reversed compatibility effects of action observation in imitation and joint action. J Exp Psychol Hum Percept Perform. 34:1493.

Van Overwalle F. 2009. Social cognition and the brain: a meta-analysis. Human brain mapping. 30:829-858.

Wager TD, Nichols TE. 2003. Optimization of experimental design in fMRI: a general framework using a genetic algorithm. NeuroImage. 18:293-309.

Wager TD, Sylvester CYC, Lacey SC, Nee DE, Franklin, M, Jonides J. 2005. Common and unique components of response inhibition revealed by fMRI. NeuroImage. 27:323-340.

Wang Y, Ramsey R, Hamilton AF de C. 2011. The control of mimicry by eye contact is mediated by medial prefrontal cortex. J Neurosci. 31:12001e12010.

Weeks DJ, Proctor RW. 1990. Salient-features coding in the translation between orthogonal stimulus and response dimensions. Journal of Experimental Psychology: General 119:355–366.

Wiggett, AJ, Hudson M, Tipper SP, Downing PE. 2011. Learning associations between action and perception: Effects of incompatible training on body part and spatial priming. Brain and Cognition, 76:87–96.

Yarkoni T, Poldrack RA, Nichols TE, Van Essen DC, Wager TD. 2011. Large-scale automated synthesis of human functional neuroimaging data. Nature methods. 8(8):665.

Zaki J, Hennigan K, Weber J, Ochsner KN. 2010. Social cognitive conflict resolution: Contributions of domain general and domain specific neural systems. Journal of Neuroscience. 30: 8481–8488.

Zaki J, Ochsner KN. 2012. The neuroscience of empathy: progress, pitfalls and promise. Nature neuroscience. 15(5):675.

Tables

Table 1. fMRI studies investigating imitation control using modified versions of the imitation inhibition task. Evidence for implication of mPFC and rTPJ is inconsistent across studies.

	Sample (Males: Females)	Dissociation of Imitative and Spatial Processes	Analysis		Brain Networks		
			ROI	Whole-Brain	ToM		MD
					mPFC	rTPJ	
Brass, Zysset, & von Cramon, 2001	10 (4:6)			✓	✓		✓
Brass, Derfuss, & van Cramon, 2005	20 (8:12)			✓	✓	✓	✓
Brass, Ruby, & Spengler,	20*		✓		✓	✓	

2009							
Spengler, von Cramon, & Brass, 2009	18 (9:9)		✓	✓	✓	✓	✓
Bien, Roebroeck, Goebel, & Sack, 2009	15 (5:10)	✓		✓			✓
Crescentini, Mengotti, Grecucci, & Rumiati, 2011	19 (9:10)	✓		✓			✓
Cross & Iacoboni, 2013	24 (12:12)	✓		✓			✓
Mengotti, Corradi	22 (10:12)	✓		✓			✓

Dell'Acqua, & Rumiati, 2012							
Cross, Torrisi, Losin, & Iacoboni, 2013	25 (5:15)	✓		✓	✓		✓
Klapper, Ramsey, Wigbouds, & Cross, 2014	19 (2:17)		✓		✓**		
Marsh, Bird, & Catmur, 2016	24 (7:17)	✓		✓			✓
Wang, Ramsey, & Hamilton,	20 (5:15)			✓	✓	✓	✓

2011

Table 1. fMRI studies in chronological order that investigated imitation control using modified versions of the imitation inhibition task. For all studies, engagement of mPFC or rTPJ is reported only for contrasts that test for inhibiting the urge to automatically imitate. Engagement (or no engagement) of the MD network is reported only for whole-brain analyses. Except for in Wang, Ramsey, & Hamilton (2011), which used hand movements, all other tasks used modified versions of the imitation inhibition tasks involving finger movements (Brass et al., 2000). For a more detailed version of this table, see Supplementary Table S6. *Number of males and females not mentioned. **mPFC showed engagement only at $p<.005$, uncorrected.

Table 2. General compatibility effect and sex*compatibility interaction for the imitation inhibition task (Experiment 1).

				MNI coordinates		
Region	Cluster Size	P FWE Corr	t-value	x	y	z
(A) GENERAL COMPATIBILITY EFFECT (Incompatible > Compatible)						
L inferior parietal lobule extending	**986**	**<0.001**	**8.40**	**-39**	**-40**	**43**
into superior parietal lobule and			**6.50**	**-36**	**-37**	**70**
superior frontal gyrus			**6.38**	**-27**	**-7**	**70**
L cerebellum	**150**	**0.001**	**5.79**	**-21**	**-55**	**-41**
			4.95	**-30**	**-55**	**-35**
			4.72	**-9**	**-70**	**-44**
R cerebellum	**198**	**<0.001**	**5.71**	**21**	**-58**	**-44**
			5.12	**45**	**-46**	**-32**
			4.32	**39**	**-55**	**-23**
R precentral gyrus extending across	**183**	**<0.001**	**5.12**	**27**	**-1**	**70**
superior and middle frontal gyri			**5.04**	**42**	**2**	**58**
			4.39	**39**	**-10**	**61**
R postcentral gyrus extending into	**481**	**<0.001**	**5.18**	**33**	**-40**	**73**
superior and inferior parietal			**4.55**	**42**	**-40**	**67**

lobules			**4.50**	**48**	**-34**	**37**
R posterior middle temporal gyrus	41	0.179	4.61	66	-46	1
			4.13	57	-40	-8
			3.63	60	-43	13
L insula	24	0.458	4.67	-36	17	-2
R posterior medial frontal cortex	20	0.564	4.79	3	-4	73
L posterior medial frontal cortex	55	0.083	4.40	-3	-1	52
			3.82	-6	11	52
R pallidum extending into thalamus	11	0.834	4.14	21	-7	-2
			3.80	15	-6	7
L paracentral lobule	11	0.834	3.89	-12	-19	79
R middle cingulate cortex	20	0.564	3.85	9	14	43
			3.78	6	8	49
			3.67	6	17	52
(B)SEX*COMPATIBILITY						
[Female (incompatible>compatible) > Male (incompatible>compatible)]						
L superior parietal lobule extending into postcentral gyrus	**93**	**0.011**	**4.98**	**-21**	**-37**	**70**
			4.80	**-30**	**-19**	**46**
			4.60	**-24**	**-31**	**52**

L cerebellum	16	0.679	4.34	-24	-55	-38
			4.04	-21	-55	-29

Table 2. Regions surviving a voxel-level threshold of p<.001 and 10 voxels are reported for the (A) general compatibility effect and (B) sex*compatibility interaction for the imitation inhibition task. Subclusters at least 8 mm from the main peak are listed. Bold font indicates clusters that survive correction for multiple corrections using a family-wise error (FWE) correction (p < .05). MNI = Montreal Neurological Institute.

Table 3. Responses in each MD network fROI for spatial and imitative compatibility.

ROI	ROI size	Inter-subject overlap	Average ROI mask size (voxels)	Spatial Compatibility			Imitative Compatibility		
				T	p-value	p-FDR	t	p-value	p-FDR
L_SPL	1173	1	117	2.00	0.026	**0.028**	1.13	0.131	0.191
L_IPS	287	1	28	2.00	0.026	**0.028**	1.96	0.028	0.089
L_IPL	641	1	64	2.72	0.005	**0.019**	2.05	0.023	0.089
L_MFG	536	1	53	2.16	0.018	**0.028**	0.53	0.301	0.324
L_PrecG	338	1	33	2.17	0.018	**0.028**	0.91	0.184	0.227
L_IFG	181	1	18	1.83	0.040	**0.037**	1.53	0.066	0.118
L_Insula	197	1	19	2.78	0.004	**0.019**	0.52	0.304	0.324
L_SMA	294	1	29	2.52	0.008	**0.020**	0.39	0.349	0.349
R_SPL	1181	1	118	2.30	0.013	**0.026**	1.56	0.062	0.118
R_IPS	227	1	22	2.03	0.024	**0.028**	2.30	0.013	0.069
R_IPL	599	1	59	2.65	0.005	**0.019**	2.50	0.008	0.063
R_MFG	535	1	53	3.57	<0.001	**0.006**	1.55	0.064	0.118
R_PrecG	269	1	26	2.43	0.009	**0.021**	1.59	0.060	0.118
R_IFG	265	1	26	2.61	0.006	**0.019**	2.53	0.007	0.063
R_Insula	184	1	18	2.09	0.021	**0.028**	1.24	0.120	0.175

R_SMA	328	1	32	2.30	0.022	**0.028**	1.06	0.148	0.198

Table 3. Responses in each MD network fROI for spatial and imitative compatibility. For each individual, for the MD network mask, the Hard>Easy contrast was used and the top 10% of voxels (based on t-values) within each parcel were defined as that individual's fROI. Uncorrected p-values as well as FDR corrected p values are reported. Cells in bold are fROIs which survive correction for multiple comparisons ($p<.05$, FDR-corrected).

Table 4. Responses in each ToM network fROI for spatial and imitative compatibility.

ROI	ROI size	Inter-subject overlap	Average ROI mask size (voxels)	Spatial Compatibility			Imitative Compatibility		
				T	p-value	p-FDR	t	p-value	p-FDR
DMPFC	576	1	57	-1.38	0.913	0.951	-1.167	0.876	0.898
MMPFC	494	1	49	-0.043	0.517	0.951	-1.081	0.857	0.898
VMPFC	382	1	38	-1.690	0.951	0.951	-1.286	0.898	0.898
RTPJ	1018	1	101	1.543	0.065	0.258	-0.106	0.542	0.898

Table 4. Responses in each ToM network fROI for spatial and imitative compatibility. For each individual, for the ToM network mask, the Belief>Photo contrast was used and the top 10% of voxels (based on t-values) within each parcel were defined as that individual's fROI. Uncorrected p-values as well as FDR corrected p values are reported. Cells in bold are fROIs which survive correction for multiple comparisons ($p<.05$, FDR-corrected).

Figure Captions

Figure 1. Sex differences in inhibitory control tasks. Females experience greater interference than males in multiple inhibitory control tasks.

	Task	Sample (Male: Female)	Trials per condition	Sex Difference – Interference	Task Requirements	Conditions	
						Compatible	Incompatible
Bayliss et al. (2005)	Gaze-cueing	80 (40:40)	144	Females > Males	Respond to letter cue		
Bayliss et al. (2005)	Arrow-cueing	40 (20:20)	144	Females > Males	Respond to letter cue		
Rubia et al. (2010)	Oddball	63 (38:25)	160 congruent, 24 oddball	Females > Males	Respond to arrow direction		
Stoet (2010)	Flanker	80 (40:40)	120	Females > Males	Respond to central circle		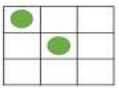
Clayson et al. (2011)	Flanker	114 (60:54)	450	Females > Males	Respond to central arrow		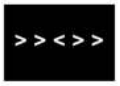
Butler et al. (2015)	Automatic Imitation	230 (97:133)	~30	Females > Males	Respond to number cue		
Stoet (2017)	Simon task	418 (236:182)	51	Females > Males	Respond to arrow direction		

Figure 1. Sex differences in inhibitory control tasks. Females experience greater interference than males in multiple inhibitory control tasks.

Images are produced based on figures and description in each experiment apart from Butler et al. (2015) which are the actual images used. Also, in Rubia et al. (2010), the sex difference showed increased interference by the oddball trials rather than the incongruent trials and this is what is represented by the images. Finally, in Butler et al. (2015), participants completed 60 trials that were 30 ± 2 trials per compatible and incompatible condition.

Figure 2. Stimuli for the imitation inhibition and functional localiser tasks.

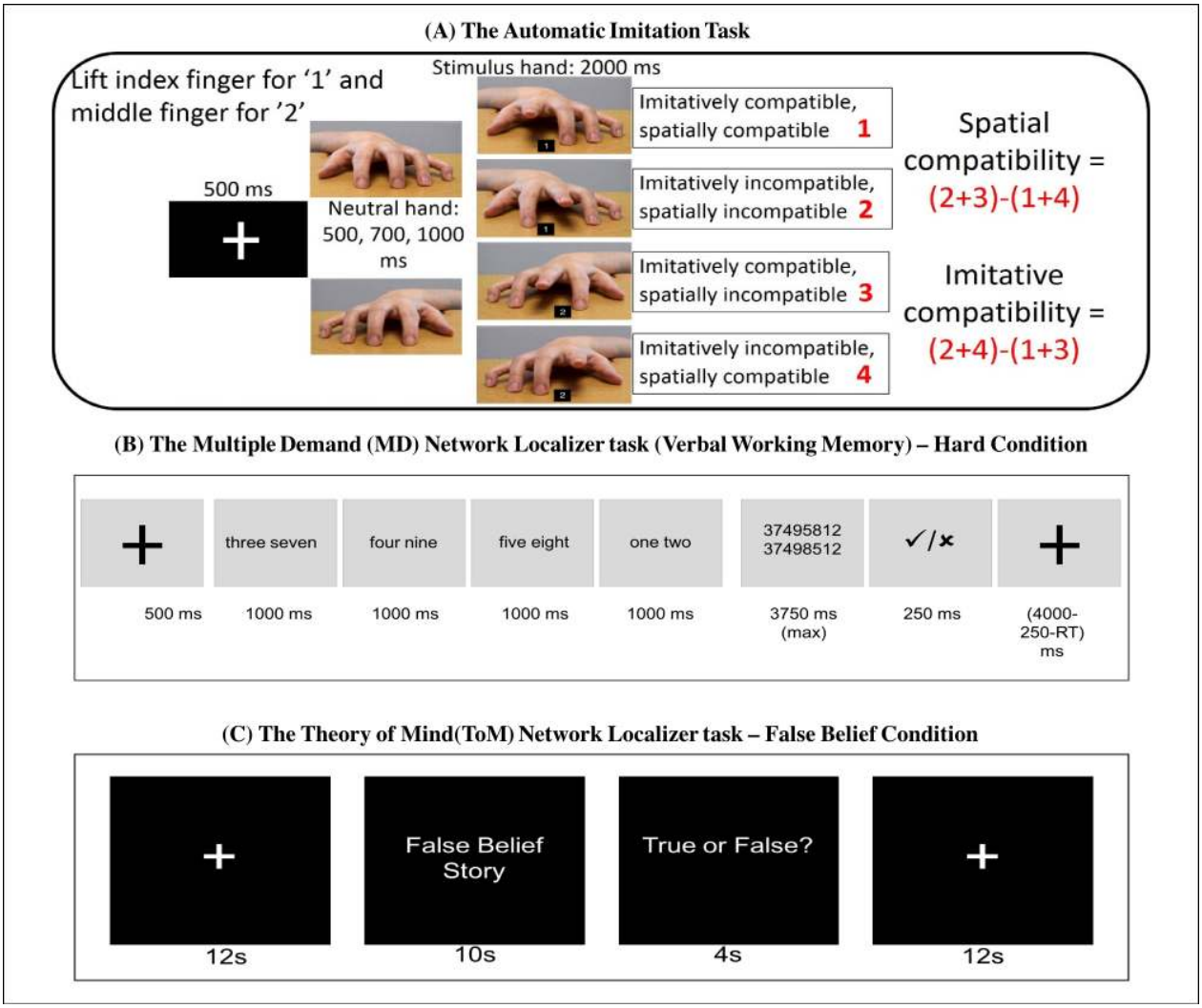

Figure 2. Stimuli for the imitation inhibition and functional localiser tasks.

Stimuli and trial design for the Imitation Inhibition task (A), the Multiple Demand Network localiser task (B), and the Theory of Mind localiser task (C).

Figure 3. The parcels used to define the MD and ToM networks.

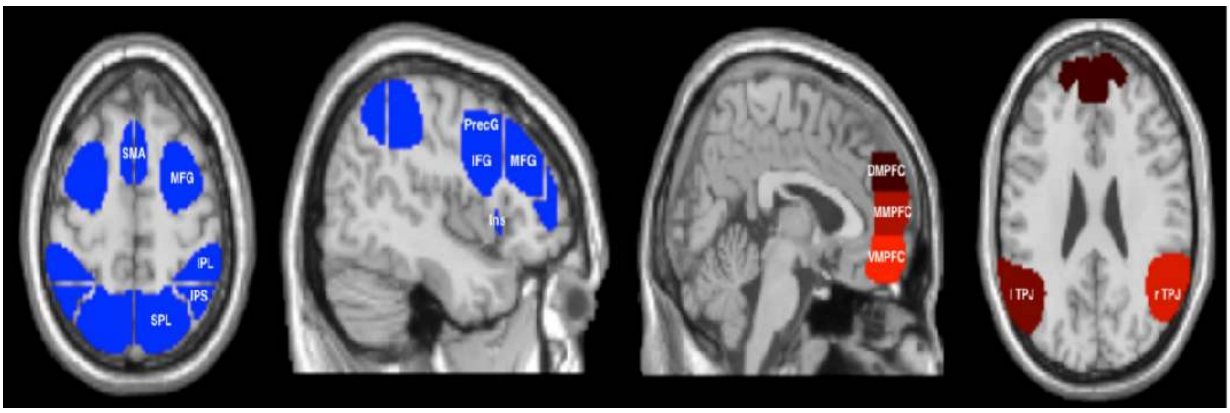

Figure 3. The parcels used to define the MD and ToM networks.

Graphical representation of the parcels used to define the MD and ToM network fROIs.

The MD network consisted in 16 parcels and the ToM network included 4 parcels.

Figure 4. General Compatibility Effect and Sex*Compatibility Interaction in the imitation inhibition task (Experiment 1).

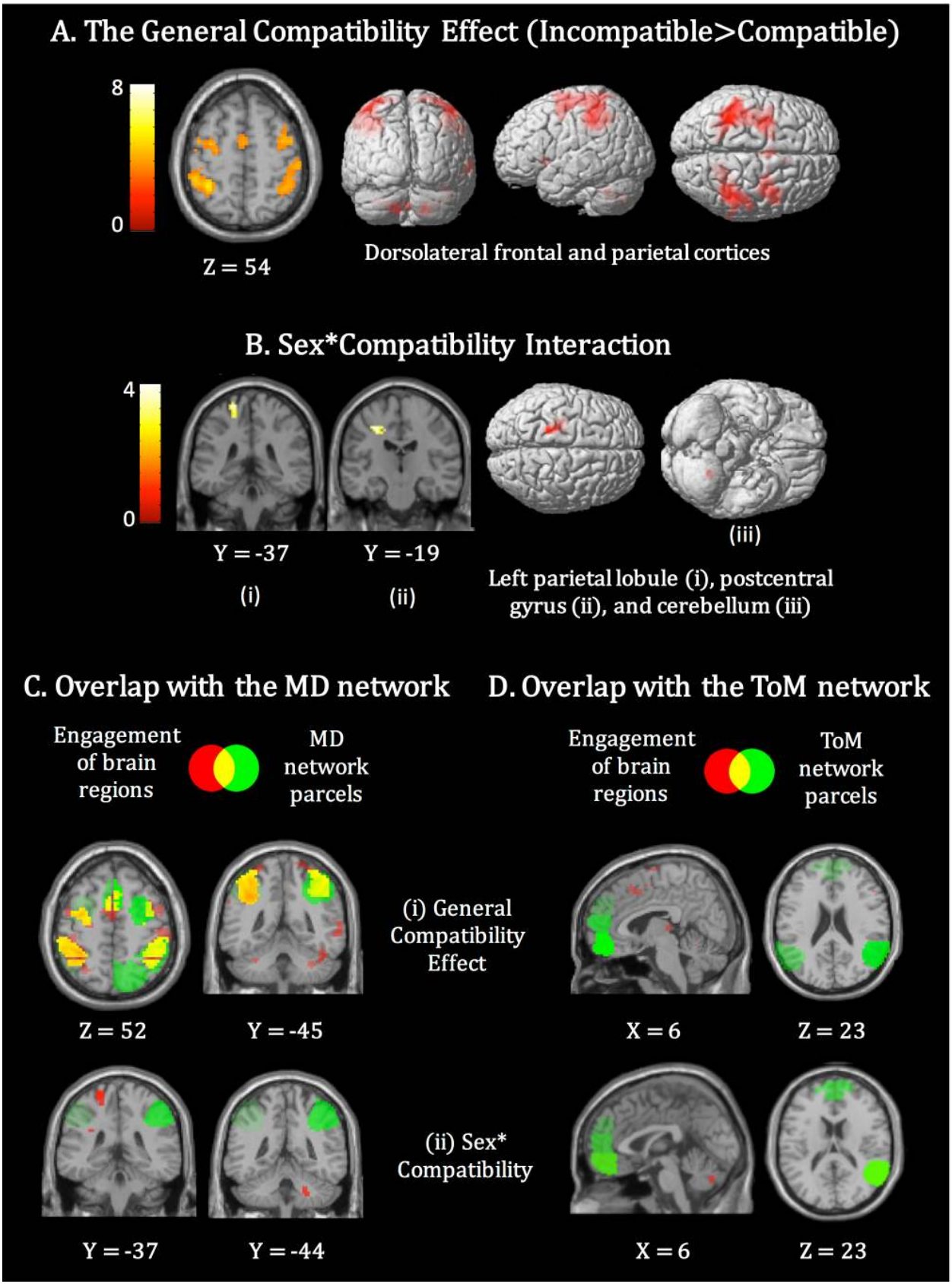

Figure 4. General Compatibility Effect and Sex*Compatibility Interaction in the imitation inhibition task (Experiment 1).

(A) Results for the General Compatibility Effect (Incompatible > Compatible). Clusters emerged in the dorsal frontoparietal cortices. (B) Results for the Sex*Compatibility Interaction (defined as [Female (Compatibility Effect)>Male (Compatibility Effect)]. Clusters emerged in the left superior parietal cortex extending into the postcentral gyrus.

Both the MD network parcels (C) and ToM network parcels (D) and general compatibility (i) and sex*compatibility (ii) contrasts are displayed on a common brain template. The overlap shows overlap between areas of the MD network and brain regions engaged by the general compatibility effect. Voxel-wise threshold used for all images was $p<.001$, $k=10$. For a complete set of results, see Table 2, and Supplementary Tables S2.1 and S2.2.

Figure 5. Behavioural Sex Differences in Imitative and Spatial Compatibility Effects

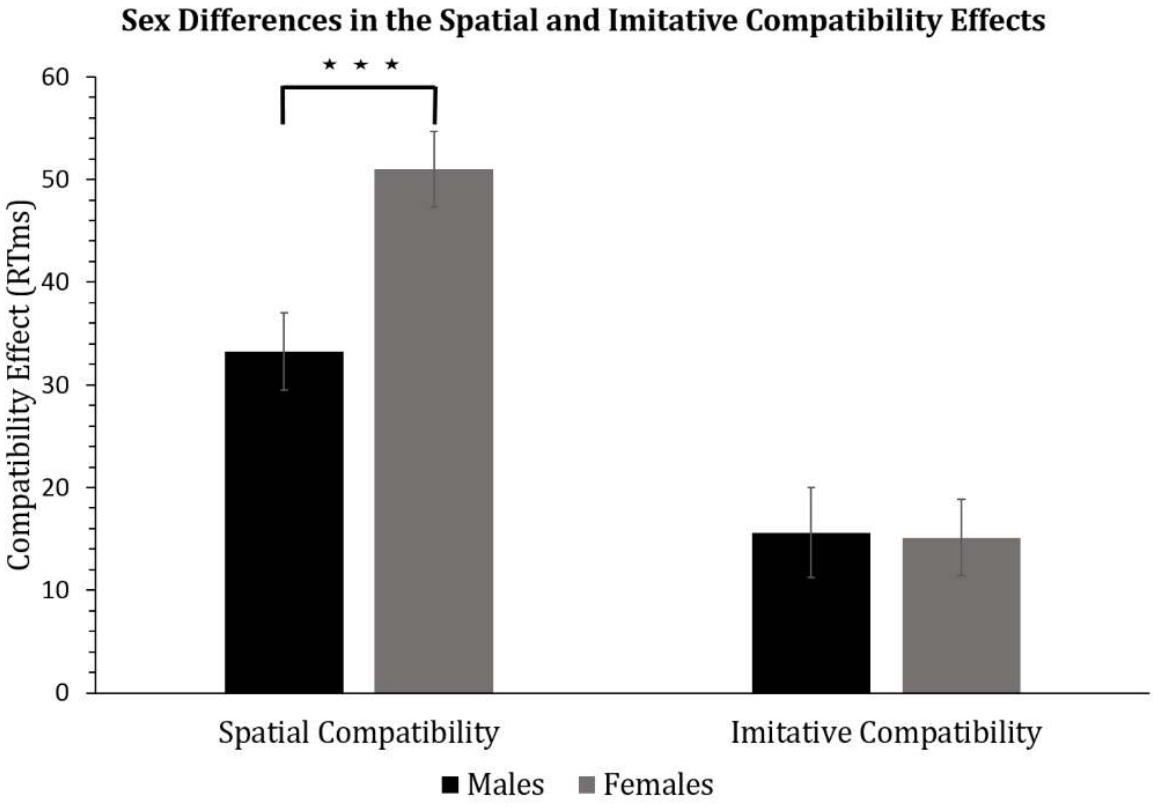

Figure 5. Behavioural Sex Differences in Imitative and Spatial Compatibility Effects

The spatial and imitative compatibility effects (RTs) in males and females in milliseconds. Error bars denote standard error of mean by participants.

Figure 6. Responses in the MD (A) and ToM (B) network fROIs for imitative and spatial compatibility effects.

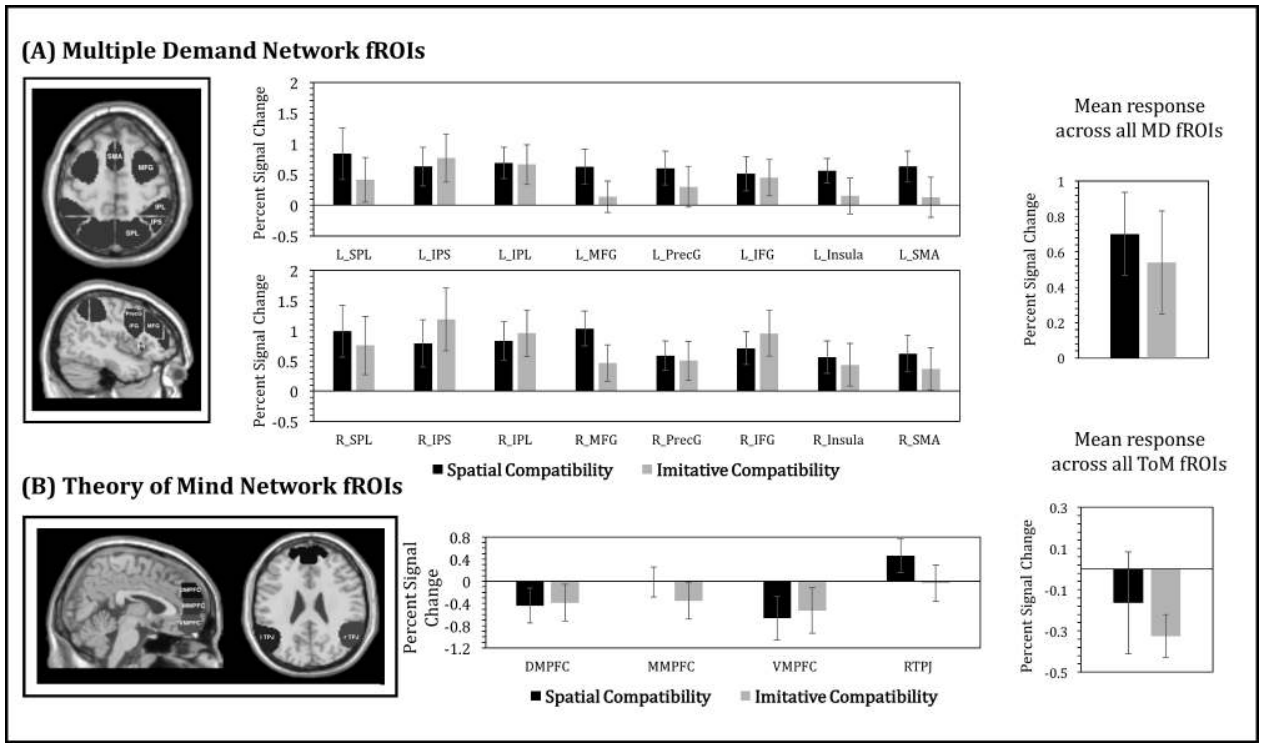

Figure 6. Responses in the MD (A) and ToM (B) network fROIs for imitative and spatial compatibility effects.

The parcels used to define individual fROIs and the responses to spatial and imitative compatibility effects in the MD (A) and ToM (B) network fROIs. Error bars denote standard error of mean by participants. All MD network fROIs were sensitive to spatial compatibility effects (FDR corrected, $p<.05$). Bilateral IPL, bilateral IPS, and the right IFG showed a significant response for imitative compatibility effects, but at an uncorrected threshold of $p<.001$.

Figure 7. Sex differences in the responses in MD network fROIs for imitative and spatial compatibility effects.

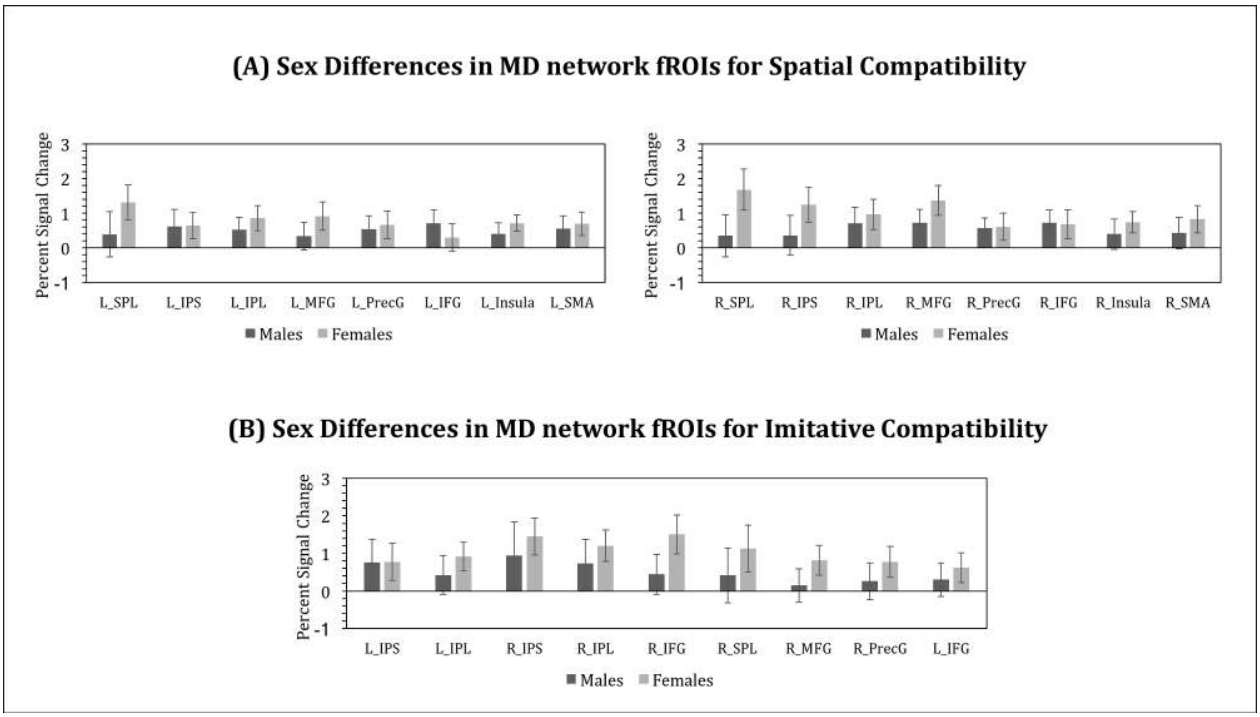

Figure 7. Sex differences in the responses in MD network fROIs for imitative and spatial compatibility effects.

Responses to spatial (A) and imitative compatibility (B) effects separately for males and females in the MD network. Error bars denote standard error of mean by participants. None of the fROIs showed a sex difference either in imitative or spatial compatibility.

Supplementary Information

Development of Stimuli

The imitation inhibition task used in Experiment 2 in the present study is a modified version of a previously existing paradigm (Brass et al., 2000; Catmur & Heyes, 2010). In order to avoid any own-sex bias, we decided to use a hand stimulus which was rated as neutral. 51 participants (19 males, $Mean_{age} = 23.49$, $SD_{age} = 3.12$) other than the ones who participated in the current study were asked to rate 18 white Caucasian hand stimuli (9 male hands, 9 female hands) on a scale of 1 to 9, with 1 being "extremely masculine," 9 being "extremely feminine" and 5 being "neutral." An average of the rating score was obtained for each hand stimulus. The hand which had an average rating closest to 5 (Mean = 5.08) was taken as the final stimulus as it was considered to be rated most "neutral" amongst all other stimuli. In the present experiment, we again asked all participants to rate the hand they saw in the imitation inhibition task on the same scale: 1 to 9, with 1 being "extremely masculine," 9 being "extremely feminine" and 5 being "neutral." The mean of the hand ratings was 5.27; thus, on average, participants perceived the hand as 'neutral.'

Table S1.1. Responses in each MD network fROI for spatial and imitative compatibility when individual contrasts were thresholded at p<.001, uncorrected.

ROI	ROI size	Inter-subject overlap	Average ROI mask size	Spatial Compatibility			Imitative Compatibility		
				t	p-value	p-FDR	t	p-value	p-FDR
L_SPL	1173	0.92	413	1.71	0.047	**0.063**	1.49	0.072	0.137
L_IPS	287	0.86	85	1.36	0.090	0.097	2.91	0.003	**0.043**
L_IPL	641	0.82	89	1.91	0.032	**0.055**	2.70	0.005	**0.043**
L_MFG	536	0.84	140	2.37	0.012	**0.035**	0.99	0.165	0.240
L_PrecG	338	0.86	103	1.76	0.043	0.062	0.33	0.371	0.396
L_IFG	181	0.74	58	0.11	0.457	0.457	0.77	0.223	0.297
L_Insula	197	0.7	48	2.45	0.010	**0.035**	0.55	0.294	0.336
L_SMA	294	0.88	86	3.00	0.002	**0.019**	0.03	0.489	0.489
R_SPL	1181	0.9	415	1.66	0.052	0.064	2.32	0.012	0.050
R_IPS	227	0.84	71	1.36	0.091	0.097	2.21	0.017	0.053
R_IPL	599	0.76	111	1.89	0.034	**0.055**	2.40	0.011	0.050
R_MFG	535	0.88	144	3.61	<0.001	**0.007**	1.80	0.039	0.093
R_PrecG	269	0.74	56	2.06	0.024	**0.048**	1.57	0.064	0.128
R_IFG	265	0.7	56	2.34	0.013	**0.035**	1.81	0.041	0.093
R_Insula	184	0.78	44	2.22	0.017	**0.037**	0.67	0.255	0.314
R_SMA	328	0.84	101	2.32	0.013	**0.034**	1.05	0.150	0.240

Table S1.1. Responses in each MD network fROI for spatial and imitative compatibility when individual contrasts were thresholded at p<.001, uncorrected. Cells in bold show fROIs which survived correction for multiple comparisons (p<.05, FDR corr.).

Table S1.2. Responses in each ToM network fROI for spatial and imitative compatibility when individual contrasts were thresholded at p<.001, uncorrected.

ROI	ROI size	Inter-subject overlap	Average ROI mask size (voxels)	Spatial Compatibility			Imitative Compatibility		
				t	p-value	p-FDR	t	p-value	p-FDR
DMPFC	576	1	0.58	-1.23	0.88	0.88	-0.09	0.54	0.82
MMPFC	494	1	0.56	-0.02	0.49	0.88	-0.56	0.71	0.82
VMPFC	382	1	0.44	-0.96	0.82	0.88	-0.93	0.82	0.82
RTPJ	1018	1	0.92	1.20	0.12	0.47	0.78	0.22	0.82

Table S2.1 Small volume correction (SVC) with MD network mask for the general compatibility effect and the sex*compatibility interaction.

Region	Cluster Size	P FWE Corr	t-value	MNI coordinates		
				x	y	z
GENERAL COMPATIBILITY (Incompatible>Compatible)						
Left inferior parietal lobule (extending into the left postcentral gyrus)	**382**	**<0.001**	**8.40**	**-39**	**-40**	**43**
			5.57	**-48**	**-40**	**61**
			5.31	**-36**	**-43**	**67**
Left intraparietal sulcus	**79**	**0.005**	**6.50**	**-36**	**-52**	**46**
			4.27	**-30**	**-61**	**49**
Left precentral gyrus	**180**	**<0.001**	**6.38**	**-27**	**-7**	**70**
			5.11	**-33**	**-4**	**52**
			4.78	**-42**	**-1**	**55**
			4.32	**-27**	**-10**	**55**
			4.22	**-39**	**-4**	**52**
Left superior parietal lobule	14	0.249	5.31	-27	-52	70
			3.95	-15	-55	73
			3.80	-12	-58	70
Right middle frontal gyrus	**86**	**0.004**	**5.12**	**27**	**-1**	**70**
			4.04	**42**	**2**	**58**
L insula	21	0.149	4.67	-36	17	-2
Right inferior parietal lobule (extending into the right intraparietal sulcus and postcentral gyrus)	**270**	**<.001**	**4.50**	**48**	**-34**	**37**
			4.47	**39**	**-46**	**67**
			4.46	**48**	**-34**	**43**
			4.41	**45**	**-43**	**64**
			4.41	**42**	**-34**	**40**
			4.39	**33**	**-37**	**37**
			4.38	**54**	**-40**	**40**
			4.35	**45**	**-40**	**52**
			4.29	**36**	**-46**	**46**
			4.28	**39**	**-46**	**52**
			4.27	**45**	**-46**	**55**
Right superior parietal lobule	29	0.086	4.40	36	-52	67
			3.97	42	-52	52
SEX*COMPATIBILITY [Female (Incompatible>Compatible) > Male (Incompatible>Compatible)]						
No suprathreshold clusters						

Table S2.1. Regions surviving a voxel-level threshold of p<.001 and 10 voxels are reported for the general compatibility effect and sex*compatibility interaction, small volume corrected using the MD mask**.** Subclusters at least 8 mm from the main peak are listed. Bold font indicates clusters that survive correction for multiple corrections using a family-wise error (FWE) correction (p < .05). MNI = Montreal Neurological Institute**.**

Table S2.2. Small volume correction (SVC) with ToM network mask for the general compatibility effect and the sex*compatibility interaction.

Region	**Cluster Size**	**P FWE Corr**	**t-value**	**MNI coordinates**		
				x	y	z
GENERAL COMPATIBILITY (Incompatible>Compatible)						
Right temporo-parietal junction (supramarginal gyrus)	10	0.124	3.60	57	-43	37
			3.54	51	-40	34
SEX*COMPATIBILITY [Female (Incompatible>Compatible) > Male (Incompatible>Compatible)]						
No suprathreshold clusters						

Table S2.2. Regions surviving a voxel-level threshold of p<.001 and 10 voxels are reported for the general compatibility effect and sex*compatibility interaction, small volume corrected using the ToM mask**.** Subclusters at least 8 mm from the main peak are listed. Bold font indicates clusters that survive correction for multiple corrections using a family-wise error (FWE) correction (p < .05). MNI = Montreal Neurological Institute**.**

Table S3. Showing Mean RT and SD for each condition of the imitation task for both males and females.

	Spatially Compatible		**Spatially Incompatible**		**Imitatively Compatible**		**Imitatively Incompatible**	
	Mean	**SD**	**Mean**	**SD**	**Mean**	**SD**	**Mean**	**SD**
Males	666.20	157.50	699.42	159.76	675.00	158.56	690.62	158.93
Females	736.94	130.34	787.83	134.19	754.88	133.91	769.99	130.65

Table S4.1. Responses in each MD network fROI for the MD network localizer contrast.

ROI	ROI size	Inter-subject overlap	Average ROI mask size (voxels)	t	p-value	p-FDR
L_SPL	1173	1	117	11.69	<.0001	**<.0001**
L_IPS	287	1	28	11.15	<.0001	**<.0001**
L_IPL	641	1	64	10.30	<.0001	**<.0001**
L_MFG	536	1	53	11.08	<.0001	**<.0001**
L_PrecG	338	1	33	10.40	<.0001	**<.0001**
L_IFG	181	1	18	9.38	<.0001	**<.0001**
L_Insula	197	1	19	12.26	<.0001	**<.0001**
L_SMA	294	1	29	14.56	<.0001	**<.0001**
R_SPL	1181	1	118	11.36	<.0001	**<.0001**
R_IPS	227	1	22	10.18	<.0001	**<.0001**
R_IPL	599	1	59	9.25	<.0001	**<.0001**
R_MFG	535	1	53	11.61	<.0001	**<.0001**
R_PrecG	269	1	26	9.43	<.0001	**<.0001**
R_IFG	265	1	26	9.13	<.0001	**<.0001**
R_Insula	184	1	18	12.43	<.0001	**<.0001**
R_SMA	328	1	32	11.38	<.0001	**<.0001**

Table S4.1. All MD network fROIs were significantly responsive to the Hard>Easy contrast and survived correction for false discovery rate ($p<.05$).

Table S4.2. Responses in each ToM network fROI for the ToM network localizer contrast.

ROI	ROI size	Inter-subject overlap	Average ROI mask size	t	p-value	p-FDR
DMPFC	576	1	57	7.097	<.001	**<.001**
MMPFC	494	1	49	7.065	<.001	**<.001**
VMPFC	382	1	38	5.704	<.001	**<.001**
RTPJ	1018	1	101	15.025	<.001	**<.001**

Table S4.2. All ToM network fROIs were significantly responsive to the Belief>Photo contrast and survived correction for false discovery rate ($p<.05$).

Table S5. Whole-brain analysis (Experiment 2).

Region	Cluster Size	P FWE Corr	t-value	MNI coordinates		
				x	y	z
(A) GENERAL COMPATIBILITY						
Left inferior parietal lobule	**333**	**<0.001**	**5.28**	**-42**	**-28**	**43**
			5.10	**-48**	**-28**	**34**
			3.91	**-30**	**-49**	**43**
Left middle frontal gyrus	**130**	**0.018**	**5.05**	**-27**	**-10**	**49**
Right inferior parietal lobule extending into the right postcentral gyrus	**437**	**<0.001**	**4.85**	**45**	**-34**	**46**
			4.81	**48**	**-25**	**43**
			4.28	**30**	**-46**	**46**
Right middle and superior gyri extending into the right posterior-medial frontal cortex	**259**	**0.001**	**4.85**	**30**	**-4**	**52**
			4.28	**21**	**-7**	**64**
			4.23	**15**	**5**	**52**
Left posterior-medial frontal	29	0.476	4.19	-9	-1	55
Right inferior frontal gyrus and right insula lobe	**96**	**0.050**	**3.87**	**42**	**2**	**19**
				48	**8**	**22**
				42	**17**	**1**
Right precuneus	36	0.374	3.77	12	-64	52
			3.56	18	-70	49
Right supramarginal gyrus	26	0.527	3.75	63	-40	31
			3.68	63	-49	28
Right cerebellum	12	0.805	3.68	36	-49	-35
(B) SPATIAL COMPATIBILITY						
Intraparietal sulcus extending into the right postcentral gyrus	**136**	**0.019**	**4.65**	**33**	**-43**	**46**
			3.87	**48**	**-25**	**43**
Bilateral posterior medial frontal	**117**	**0.033**	**4.55**	**-6**	**-1**	**55**
			4.22	**9**	**5**	**52**
			3.48	**-9**	**5**	**46**
Left precentral gyrus	26	0.538	4.49	-57	5	31
Left precentral gyrus	68	0.139	4.34	-24	-16	58
			4.28	-27	-10	52
Right precentral gyrus	27	0.521	4.30	63	8	28

Right insula lobe	46	0.282	4.23	39	14	1
Right superior frontal gyrus	122	0.028	4.16	27	-7	58
			4.15	27	-7	49
Left inferior parietal lobule	**75**	**0.025**	**3.95**	**-36**	**-37**	**40**
			3.66	**-48**	**-31**	**40**
Left insula lobe	17	0.702	3.92	-33	14	7
Left postcentral gyrus	13	0.780	3.69	-63	-16	34
Right precuneus	22	0.607	3.67	12	-70	46
			3.60	12	-61	46
	10	0.838	3.39	57	-16	22
(C) IMITATIVE COMPATIBILITY						
Right supramarginal gyrus and right postcentral gyrus	40	0.349	3.76	45	-34	43
			3.64	42	-34	55
Left inferior parietal lobule	15	0.666	3.50	-42	-28	40
(D) SEX*COMPATIBILITY (GENERAL)						
Right superior occipital gyrus	10	0.845	3.48	30	-67	28
(E) SEX*COMPATIBILITY (SPATIAL)						
Right superior occipital gyrus	10	0.838	3.65	33	-64	31
(F) SEX*COMPATIBILITY (IMITATIVE)						
No suprathreshold clusters						

Table 5. Regions surviving a voxel-level threshold of p<.001 and 10 voxels are reported for (A) general compatibility (B) spatial compatibility (C) imitative compatibility effects and sex*compatibility interactions separately for (D) general (E) spatial and (F) imitative compatibility effects. Subclusters at least 8 mm from the main peak are listed. Bold font indicates clusters that survive correction for multiple corrections using a family-wise error (FWE) correction ($p < .05$). MNI = Montreal Neurological Institute.

Table S6. Detailed table of fMRI studies using the imitation inhibition task and the contributions of ToM and MD networks in imitation inhibition.

	Sample		No. of trials per condition	Design	Task Instructions	ROI/Whole brain		Regions			Thresholding
	M:F	Age		Block/ Event-related		ROI	WB	mPFC	rTPJ	MD	
1. Brass, Zysset, & von Cramon, 2001	10 (4:6)	23.5	80 congruent, 80 incongruent	Mixed	**Block1: tap index finger** **Block2: lift index finger**		Y	Y (Frontopolar cortex, BA 10)	N	Y (MFG, Cuneus, Anterior parietal cortex)	p<.001, uncorrected
2. Brass, Derfuss, & von Cramon. 2005	20 (8:12) – 10 for Imi, 10 for Stroop	26	40 congruent, 40 incongruent, 40 baseline, 40 null	Event-related	Index finger for '1' Middle finger for '2'		Y	Y aFMC	Y (BA40)	Y	p<.001, uncorrected
3. Brass, Ruby, & Spengler, 2009	20		35 simultaneous congruent, 35 simultaneous incongruent, 35 delayed congruent, 35 delayed incongruent,	Mixed	Same as above Simultaneous: number cue appeared with irrelevant hand Delayed: response led to appearance of irrelevant hand	Y		Y (for simultaneous incongruent > congruent only)*	Y (for simultaneous incongruent > congruent only)*		P<.001, uncorrected
4. Spengler, von	18 (9:9)	25	72 incongruent, 72 congruent, 36 null	Event-related	Same as 2.	Y**		Y (overlap with	Y (overlap with	Y (see supple-	P<.05, corrected for

	Cramon, & Brass, 2009								self-referential and ToM tasks; -ve correlation with RT interference)	agency and ToM tasks)	mentary material: SII, MFG)	multiple comparisons
5.	Bien, Roebroeck, Goebel, & Sack, 2009	15 (5:10)	23	64 imitative congruent, 64 imi incongruent, 64 spat congruent, 64 spat incongruent	Mixed	**Block 1: imitate finger movement (imitative trials) Block2: follow spatial cue for movement (spatial trials)**		Y	N	N	Y*** (premotor cortex, bilateral posterior parietal and frontal /parietal opercular cortex, right STS)	P<.045, cluster size threshold = 50
6.	Crescentini, Mengotti, Grecucci, & Rumiati, 2011	19 (9:10)	24.6	60 biological congruent, 60 bio incongruent, 60 non-bio congruent, 60 non-bio incongruent	Mixed	**Modified version of 1. With biological (human hand) and non-biological (white dot) stimuli; but ppts responded after movement offset instead of onset**		Y	N	N	Y (only right Insula)	P<.05, corrected for multiple comparisons
7.	Cross & Iacoboni, 2013	24 (12:12)			Mixed	Block1: imitate finger movements Block2: imitate spatial dot movement		Y	N	N	N	P<.05, FWE corrected
8.	Mengotti, Corradi-Dell'Acqua, & Rumiati, 2012	22 (10:12)	24.4	80 per condition	Mixed	**Task1: tap anatomical finger Task2: tap finger on same side of space**		Y	N	N/Y (for only AN_NS over all others i.e. for the condition 'imi comp + spat incomp')	Y****	P<.05 FWE
9.	Cross, Torrisi,	25 (5:15);	19-39	80 imi congruent, 80 imi incongruent, 80	Block	**Block1: lift index finger on finger**		Y	Y	N	Y (ACC, bilateral insula extending	P<.05, FWE corrected

Losin, & Iacoboni, 2013	20 included in analysis		spat cong, 80 spat incong, 80 nulls		**movement Block 2: lift middle finger on finger movement Block ¾: lift index/middle finger when dot moves**					into frontal pole and orbitofrontal cortex, IFG, PrecG, SPL)	
10. Klapper, Rasey, Wigboldus, & Cross, 2014	19 (2:17)	21.95	160 congruent, 160 incongruent	Event related	Index for '1' Middle for '2'	Y	Y	Y (at p<.005, uncorrected: incong>cong, human>non-human)	N/Y (at p<.005, uncorr for human>non-human) and 3-way cong x form x belief at p<.05 FWE corr		
11. Marsh, Bird, & Catmur, 2016	24 (7:17)	23.71	80 imi cong, 80 imi incong, 80 spat cong, 80 spat incong	Event related	Lift index for '1' Lift middle for '2'		Y	N	N	Y (IFG, IPL, ACC); also left TPJ	P<.05, FWE corrected
12. Wang, Ramsey, & Hamilton, 2011	20 (5:15)	23	96 congruent (averted + direct gaze), 96 incongruent, 54 catch trials	Mixed	**Block1: Hand open Block2: Hand closed**		Y	Y (for averted incong > cong)	Y (for averted incong > cong)	Y (main effect:IPL, Cuneus); (averted: MOG, MTG, STS, temporal pole, IFG, precuneus, MFG, SPL, PMC, IPL, cuneus)	P<.05, FWE corrected